*Organometallics* **1993,** *12,* 3705-3723

# Monomeric and Dimeric Zirconocene Imido Compounds: Synthesis, Structure, and Reactivity

Patrick J. Walsh, Frederick J. Hollander, and Robert G. Bergman*

*Department of Chemistry, University of California, Berkeley, Berkeley, California 94720*

*Received March 9, 1993*[⊗]

This paper outlines the generation of the transient monomeric imido complexes $Cp_2Zr{=}NR$ (**1a–e**), their successful trapping with unsaturated organic molecules and dative ligands, and their use in activating C—H bonds. The generation of $Cp_2Zr{=}NR$ has been accomplished by thermolysis of the alkyl amides $Cp_2Zr(NHR)(R')$ (**2a–d**) and bis(amides) $Cp_2Zr(NHR)_2$ (**3a–c**) via $\alpha$-abstraction of alkane and amine, respectively. The imido intermediate **1a**, generated from alkyl amide **2a** (R = 4-*tert*-butylphenyl, R′ = Me) in THF, resulted in the formation of the bridging imido dimer **4a** in 70% yield. In contrast, the generation of intermediates **1b–d** (**1b** R = *tert*-Bu; **1c** R = 2,6-dimethylphenyl; **1d** R = $Si(CMe_3)Me_2$) under similar conditions furnished the monomeric imido THF complexes **5b–d** in 71, 69, and 72% yields. Imido dimer **4a** and monomer **5b** were characterized crystallographically. The THF ligands of **5b–d** are weakly bound, as demonstrated by the exchange of bound and free THF in **5c** on the NMR time scale and by facile substitution of $Ph_3PO$ for THF in **5b**, giving the triphenylphosphine oxide adduct $Cp_2Zr(NCMe_3)(OPPh_3)$ (**6b**). Thermolysis of the alkyl amides **2b** and **2d** at 85–95 °C in benzene resulted in the addition of the C—H bond of benzene across the Zr—N linkage to provide the phenyl amides **7b** and **7d**. Similarly, the THF adduct **5b** reacted with benzene under the same conditions to give the C—H activation product **7b**. The imido intermediates $Cp_2Zr{=}NR$ undergo cycloaddition reactions with a variety of unsaturated organic compounds. In addition to formation of azametallacyclobutenes (e.g., **8b**, **8c**, **9c**, **10b**) from alkynes, certain olefins react with $Cp_2Zr{=}NR$ to give azametallacyclobutanes. Thus, upon reaction of norbornene or ethylene with imido complex **5b** an equilibrium mixture of **5b**, free olefin, free THF, and the metallacycles **12b** and **13b**, respectively, were observed. Addition of a large excess of norbornene shifted the equilibrium almost entirely to the azametallacyclobutane **12b** and facilitated its isolation. The structure of **12b** was determined after crystallization from hexamethyldisiloxane. Complex **5b** also reacted with benzophenone and *tert*-butyl isocyanate to provide the *tert*-butylimine of benzophenone and di-*tert*-butylcarbodiimide in 89 and 65% yields, respectively. Monomer **5b** reacted with *tert*-butyl isocyanide to provide the coupling/trapping product $Cp_2Zr(N(CMe_3)C{=}NCMe_3)(CNCMe_3)$ (**16**), while reaction of **5b** with isobutene oxide gave the epoxide-opened product $Cp_2Zr(NHCMe_3)(OCH_2C(Me){=}CH_2)$ (**17**). Finally, heating the alkyl amide $Cp_2Zr(NHCHPh_2)(CH_2CH_2CMe_3)$ (**2e**) (which contains hydrogens both $\alpha$ and $\beta$ to nitrogen) with diphenylacetylene yielded the azametallacyclobutene product formed via $\alpha$-abstraction in 64% yield.

## Introduction

Certain mononuclear imido complexes of group IV metals have recently been found to display unique reactivity.[1-4] These complexes readily activate $sp^2$ and in some cases $sp^3$ hybridized C–H bonds (e.g., benzene[1] and methane[2]) and will undergo 2 + 2 cycloaddition reactions with alkynes.

We now report the full details of our earlier communication[1] along with further exploration of the chemistry of zirconocene imido complexes, $Cp_2Zr{=}NR$ (**1a–e**).[5] We have found evidence which suggests that the ability of the $Zr{=}NR$ functionality to activate C—H bonds is related to the nature of the R group. We have also extended $Cp_2Zr{=}NR$ cycloaddition reactions to olefins, isocyanates, and ketones.

## Results

**Synthesis of Zirconocene Alkyl Amide and Bis(amide) Complexes.** Among the methods for the synthesis of transition metal amide complexes the metathesis of transition metal halides with alkali metal amides works quite well for early metals.[6] Addition of the primary lithium amides LiNHR to zirconocene alkyl chlorides $Cp_2Zr(R')(Cl)$ (R′ = Me,[7] $CH_2CH_2CMe_3$[8]) and the dichloride

---

[⊗] Abstract published in *Advance ACS Abstracts*, August 15, 1993.

(1) (a) Walsh, P. J.; Hollander, F. J.; Bergman, R. G. *J. Am. Chem. Soc.* **1988,** *110,* 8729. (b) Walsh, P. J. Ph.D. Thesis, University of California, Berkeley, 1990.

(2) (a) Cummins, C. C.; Baxter, S. M.; Wolczanski, P. T. *J. Am. Chem. Soc.* **1988,** *110,* 8731. (b) Cummins, C. C.; Schaller, C. P.; Van Duyne, G. D.; Wolczanski, P. T.; Chan, A. W. E.; Hoffmann, R. *J. Am. Chem. Soc.* **1991,** *113,* 2985.

(3) For group IV imido complexes which are exceptions to this see: (a) Hill, J. E.; Porfilet, R. D.; Fanwick, P. E.; Rothwell, I. P. *Angew. Chem., Int. Ed. Engl.* **1990,** *29,* 664. (b) Roesky, W. H.; Voelker, H.; Witt, M.; Noltemeyer, M. *Angew. Chem., Int. Ed. Engl.* **1990,** *29,* 669. (c) Profilet, R. D.; Zambrano, C. H.; Fanwick, P. E.; Nash, J. J.; Rothwell, I. P. *Inorg. Chem.* **1990,** *29,* 4364.

(4) Nugent, W. A.; Mayer, J. A. *Metal-Ligand Multiple Bonds*; Wiley-Interscience: New York, 1988.

(5) Throughout this paper the Zr—N imido linkage is drawn as a double bond for clarity (e.g., $Cp_2Zr{=}NR$). The nature of this bond is discussed in the text.

(6) Lappert, M. f.; Power, P. P.; Sanger, A. R.; Sruvastava, R. C. *Metal and Metalloid Amides*; John Wiley & Sons: New York, 1980.

(7) Wailes, P. C.; Weigold, H.; Bell, A. P. *J. Organomet. Chem.* **1971,** *33,* 181.

0276-7333/93/2312-3705$04.00/0

Scheme I

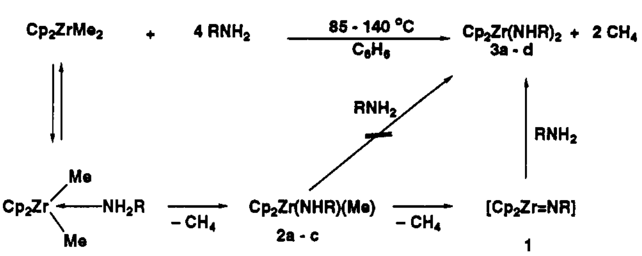

$Cp_2ZrCl_2$ resulted in the high yield synthesis of the alkyl amide $Cp_2Zr(R')(NHR)$ (**2a–e**)[9] and bis(amide) $Cp_2Zr(NHR)_2$ (**3a** and **3c**) complexes, respectively, as illustrated in eqs 1 and 2.[10]

$$Cp_2Zr(R')(Cl) + LiNHR \xrightarrow[THF]{25\ °C} Cp_2Zr(NHR)(R') + LiCl \quad (1)$$

| | R | R' | Yield |
|---|---|---|---|
| 2a | $4\text{-}CMe_3\text{-}C_6H_4$ | Me | 51 % |
| 2b | $CMe_3$ | Me | 90 % |
| 2c | $2,6\text{-}Me_2\text{-}C_6H_3$ | $CH_2CH_2CMe_3$ | 72 % |
| 2d | $Si(CMe_3)Me_2$ | $CH_2CH_2CMe_3$ | 72 % |
| 2e | $CHPh_2$ | $CH_2CH_2CMe_3$ | 74 % |

$$Cp_2ZrCl_2 + 2\ LiNHR \xrightarrow[THF]{25\ °C} Cp_2Zr(NHR)_2 + 2\ LiCl \quad (2)$$

| | R | Yield |
|---|---|---|
| 3a | $4\text{-}CMe_3\text{-}C_6H_3$ | 83 % |
| 3c | $2,6\text{-}Me_2\text{-}C_6H_3$ | 71 % |

A complementary route to the bis(amides) **3a–d** involved thermolysis of $Cp_2ZrMe_2$[11] in toluene with excess amine (Scheme I). Reaction of $Cp_2ZrMe_2$ with either 4-*tert*-butylaniline (105 °C, 72 h), *tert*-butylamine (140 °C, 96 h), 2,6-dimethylaniline (140 °C, 48 h), or (*tert*-butyldimethylsilyl)amine (140 °C, 72 h) gave the bis(amides) **3a–d** in 83, 61, 84, and 68% recrystallized yields, respectively. When the reactions were conducted in sealed NMR tubes in $C_6D_6$, methane was identified by $^1H$ NMR spectrometry ($\delta$ 0.15 ppm). When 4-*tert*-butylaniline was heated with $Cp_2ZrMe_2$ at 85 °C, the methyl amide complex $Cp_2Zr(Me)(NH\text{-}4\text{-}CMe_3C_6M_4)$ (**2a**) was detected by $^1H$ NMR spectrometry before loss of the second equivalent of methane occurred. In the case of the more sterically encumbered amines *tert*-butylamine, 2,6-dimethylaniline, or (*tert*-butyldimethylsilyl)amine the methyl amides were not observed by $^1H$ NMR spectrometry but are presumed to be intermediates in these cases as well. Consistent with this postulate, heating the methyl amides **2a–2c** to 85 °C with the corresponding amine provided the bis(amides) **3a–c** all in >95% yield ($^1H$ NMR) (Scheme I). Heating alkyl amide **2a** in the presence of 1.87, 3.97, and 5.58 equiv of 4-*tert*-butylaniline and monitoring the rates of reaction by $^1H$ NMR spectrometry gave rate constants of 4.97, 5.10, and $4.76 \times 10^{-5}\ s^{-1}$, respectively, indicating that the reaction was cleanly first order in **2a** and independent of the concentration of amine. In the case of the bis(amides) **3b** and **3d** the synthesis from $Cp_2ZrMe_2$ and the corresponding amine was the method of choice; the reaction of the lithium amides with zirconocene dichloride led only to intractable products.

Scheme II

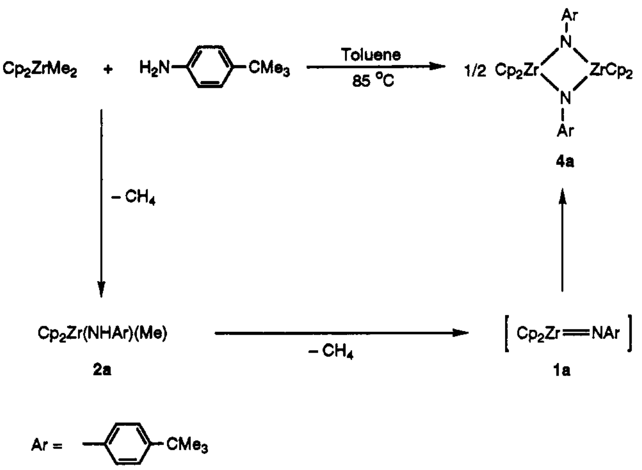

**Generation, Dimerization, and Ligation of $Cp_2Zr{=}NR$. X-ray Structure Determination of the Imido Dimer 4a and the Monomer 5b.** Thermolysis of either the alkylamide or the bis(amide) complexes led to extrusion of the alkane R'H or the amine $RNH_2$, respectively, to generate the transient intermediate $Cp_2Zr{=}NR$ (**1**), which was subsequently trapped with various unsaturated organic molecules and Lewis bases. In the case of the bis(amide) complexes, $\alpha$-abstraction of the amine is reversible which limits the range of possible trapping reagents because of competition of the liberated amine for the intermediate $Cp_2Zr{=}NR$ to regenerate the bis(amide) complex. However $\alpha$-abstraction of the alkanes R'H from the alkylamide complexes was found to be irreversible and therefore these materials proved to be of more general utility in the generation and trapping of the imido intermediates.

Heating the methyl amide **2a** to 105 °C for 48 h (Scheme II) in benzene or THF resulted in formation of methane (identified by $^1H$ NMR spectrometry, $\delta$ 0.15 ppm in $C_6D_6$) and the kelly-green bridging imido dimer **4a** in >98% yield, as judged by $^1H$ NMR integration against an internal standard. This reaction presumably proceeds via the transient imido intermediate $Cp_2Zr{=}N(4\text{-}CMe_3\text{-}C_6H_4)$ (**1a**). Alternatively, reaction of $Cp_2ZrMe_2$ with 1.0 equiv of 4-*tert*-butylaniline in toluene at 85 °C for 3 days (Scheme II) provided dimer **4a** in 70% isolated yield as large hexagonal crystals which formed as the solution was cooled to room temperature. The methylamide **2a** was identified as an intermediate in this transformation by $^1H$ NMR spectrometry when the reaction was run in a sealed NMR tube. Once crystallized, complex **4a** was not soluble in most common organic solvents; however it was slightly soluble in pyridine. The $^1H$ NMR spectrum (pyridine-$d_5$) contained singlets for the *tert*-butyl (1.37 ppm) and cyclopentadienyl groups (6.66 ppm) as well as doublets for the aromatic protons (6.02 and 7.27 ppm).

To verify the proposed connectivity of this complex, crystals of **4a** were subjected to an X-ray diffraction study. X-ray data were collected at 25 °C under the conditions

---

(8) (a) Carr, D. B.; Schwartz, J. *J. Am. Chem. Soc.* **1979**, *101*, 3521. (b) Hart, D. W.; Schwartz, J. *J. Am. Chem. Soc.* **1974**, *96*, 5115.

(9) Throughout this paper compounds have been assigned letters based on the organic moiety attached to nitrogen. For example, all compounds whose numbers contain an a are substituted with the *N*-4-*tert*-butylphenyl group. Similarly, compound numbers followed by b indicate the presence of a *tert*-butyl substituent, etc.

(10) (a) Walsh, P. J.; Baranger, A. M.; Bergman, R. G. *J. Am. Chem. Soc.* **1992**, *114*, 1708. (b) Baranger, A. M.; Walsh, P. J.; Bergman, R. G. *J. Am. Chem. Soc.* **1993**, *115*, 2753.

(11) Wailes, P. C.; Weigold, H.; Bell, A. P. *J. Organomet. Chem.* **1972**, *34*, 155.

**Table I. Crystal and Data Collection Parameters**[a]

| | 4a | 5b | 12b |
|---|---|---|---|
| temp (°C) | 25 | 25 | –95 |
| empirical formula | $C_{40}H_{56}N_2Zr_2$ | $C_{18}H_{27}NOZr$ | $C_{21}H_{27}NZr$ |
| fw | 839.5 | 364.6 | 384.7 |
| crystal size (mm) | 0.20 × 0.20 × 0.30 | 0.19 × 0.22 × 0.56 | 0.26 × 0.40 × 0.43 |
| space group | $P2_1/n$ | *Pnma* | *C*2/*c* |
| *a* (Å) | 13.4185(16) | 17.341(2) | 31.114(7) |
| *b* (Å) | 9.3796(13) | 11.5520(12) | 8.653(1) |
| *c* (Å) | 16.9932(23) | 9.3231(13) | 14.314(2) |
| $\alpha$ (deg) | 90.0 | 90.0 | 90.0 |
| $\beta$ (deg) | 107.224(10) | 90.0 | 109.50(1) |
| $\gamma$ (deg) | 90.0 | 90.0 | 90.0 |
| $V$ (Å$^3$) | 2042.9(9) | 1867.7(8) | 3633.0(21) |
| *Z* | 2 | 4 | 8 |
| $d_{calc}$ (g cm$^{-3}$) | 1.36 | 1.30 | 1.41 |
| $\mu_{calc}$ (cm$^{-1}$) | 5.3 | 5.8 | 5.9 |
| no. of reflns measd | $+h,+k,\pm l$ | $+h,\pm k,+l$ | $+h,-k,\pm l$ |
| scan width (deg) | $\Delta\theta = 0.60 + 0.35 \tan\theta$ | $\Delta\theta = 0.55 + 0.35 \tan\theta$ | $\Delta\omega = 0.65 + 0.35 \tan\theta$ |
| scan speed (deg/min) | $0.72 \rightarrow 6.70$ ($\theta$) | $0.66 \rightarrow 6.70$ ($\theta$) | 6.70 ($\omega$) |
| setting angles[b] (deg) | 26–30 ($2\theta$) | 28–30 ($2\theta$) | 26–30 ($2\omega$) |

[a] Parameters common to all structures: radiation, Mo K$\alpha$ ($\lambda$ = 0.710 73 Å); monochromator, highly-oriented graphite ($2\theta$ = 12.2°); detection, crystal scintillation counter, with PHA; $2\theta$ range, (**4a**) $3 \rightarrow 45°$, (**5b** and **12b**) $2 \rightarrow 45°$; scan type; $\theta$–$2\theta$ for **4a** and **5b**, $\omega$ for **12b**; background, measured over 0.25($\Delta\theta$) for **4a** and **5b**, and 0.25($\Delta w$) for **12b** added to each end of the scan; vertical aperture = 3.0 mm and horizontal aperture = 2.0 + 1.0 tan $\theta$ mm for **4a** and **5b**; vertical aperature = 4.0 mm and horizontal aperture = 2.0 + 1.0 tan $\theta$ mm for **12b**; intensity standards, measured every 1 h of X-ray exposure time; orientation, three reflections were checked after every 200 measurements. Crystal orientation was redetermined if any of the reflections were offset from their predicted positions by more than 0.1°. Reorientation was required twice for **5b**. [b] Unit cell parameters and their esd's were derived by a least-squares fit to the setting angles of the unresolved Mo K$\alpha$ components of 24 reflections with the given $2\theta$ range. In this and all subsequent tables the esd's of all parameters are given in parentheses, right-justified to the least significant digit(s) of the reported value.

**Table II. Selected Intramolecular Distances (Å) and Esd's for Complex 4a**

| | | | |
|---|---|---|---|
| Zr–Zr | 3.198(1) | C4–C5 | 1.371(4) |
| Zr–N | 2.093(2) | C4–C7 | 1.556(4) |
| Zr–N | 2.098(2) | C5–C6 | 1.408(4) |
| Zr–Cp11 | 2.532(7) | C7–C8 | 1.576(7) |
| Zr–Cp11′ | 2.534(8) | C7–C8′ | 1.478(10) |
| Zr–Cp12 | 2.522(3) | C7–C9 | 1.639(9) |
| Zr–Cp13 | 2.554(4) | C7–C9′ | 1.449(10) |
| Zr–Cp14 | 2.561(3) | C7–C10 | 1.350(9) |
| Zr–Cp15 | 2.544(3) | C7–C10′ | 1.747(8) |
| Zr–Cen1 | 2.257 | Cp11–Cp12 | 1.125(8) |
| Zr–Cp16 | 2.603(6) | Cp11–Cp13 | 1.042(7) |
| Zr–Cp16′ | 2.596(6) | Cp11′–Cp14 | 1.045(8) |
| Zr–Cp17 | 2.569(3) | Cp11′–Cp15 | 1.006(8) |
| Zr–Cp18 | 2.561(3) | Cp12–Cp15 | 1.390(6) |
| Zr–Cp19 | 2.565(3) | Cp13–Cp14 | 1.366(7) |
| Zr–Cp20 | 2.558(3) | Cp16–Cp18 | 1.121(7) |
| Zr–Cen2 | 2.273 | Cp16–Cp19 | 1.154(8) |
| N–C1 | 1.409(3) | Cp16′–Cp17 | 1.158(7) |
| C1–C2 | 1.376(4) | Cp16′–Cp20 | 1.134(7) |
| C1–C6 | 1.368(4) | Cp17–Cp18 | 1.339(6) |
| C2–C3 | 1.376(4) | Cp19–Cp20 | 1.336(6) |
| C3–C4 | 1.372(4) | | |

**Table III. Intramolecular Bond Angles (deg) and Esd's for Complex 4a**

| | | | |
|---|---|---|---|
| Cen1–Zr–N | 110.17 | C4–C7–C8 | 108.6(3) |
| Cen2–Zr–N | 110.93 | C4–C7–C8′ | 111.9(4) |
| Cen1–Zr–N | 111.93 | C4–C7–C9 | 107.2(3) |
| Cen2–Zr–N | 110.97 | C4–C7–C9′ | 111.5(4) |
| Cen1–Zr–Cen2 | 123.95 | C4–C7–C10 | 113.0(4) |
| N–Zr–N | 80.56(7) | C4–C7–C10′ | 105.3(3) |
| Zr–N–C1 | 130.83(15) | Cp12–Cp11–Cp13 | 118.0(7) |
| Zr–N–C1 | 129.72(15) | Cp14–Cp11′–Cp15 | 119.3(9) |
| N–C1–C2 | 122.63(22) | Cp11–Cp12–Cp15 | 117.6(5) |
| N–C1–C6 | 122.60(22) | Cp11–Cp13–Cp14 | 120.5(6) |
| C6–C1–C2 | 114.77(23) | Cp11′–Cp14–Cp13 | 121.8(6) |
| C1–C2–C3 | 123.4(3) | Cp11′–Cp15–Cp12 | 121.8(6) |
| C2–C3–C4 | 121.7(3) | Cp18–Cp16–Cp19 | 111.7(6) |
| C3–C4–C5 | 116.3(3) | Cp17–Cp16′–Cp20 | 111.7(6) |
| C3–C4–C7 | 121.7(3) | Cp16′–Cp17–Cp18 | 122.2(5) |
| C5–C4–C7 | 121.9(3) | Cp16–Cp18–Cp17 | 126.1(5) |
| C4–C5–C6 | 121.1(3) | Cp16–Cp19–Cp20 | 122.8(6) |
| C5–C6–C1 | 122.6(3) | Cp16′–Cp20–Cp19 | 125.3(5) |

outlined in Table I. The structure was solved by Patterson methods and refined by standard least-squares and Fourier techniques. Structural refinement is described in the Experimental Section with details of the structure determination. Relevant bond lengths and bond angles are listed in Tables II and III. The ORTEP diagram of **4a** shown in Figure 1 illustrates the dimeric structure of this complex. The imido bridges are symmetric, as predicted for bridging imido complexes incorporating d$^0$ metal centers.[12] Although the cyclopentadienyl ligands, the *tert*-butyl groups, and a toluene of solvation were disordered (see Experimental Section) the central imido bridges were well behaved. The Zr–N distances of 2.098(2) and 2.093(2) Å as well as the N–Zr–N angle of 80.56(7)° are typical of zirconium bridging imido dimers.[13]

Although heating **2a** in THF resulted in formation of the dimer **4a**, heating **2b** (85 °C, 42 h), **2c** (85 °C, 10 days), and **2d** (85 °C, 28 h) in THF led instead to the monomeric THF-trapped imido complexes Cp$_2$Zr(NR)(THF) (**5b–d**) in 71, 69, and 72% yields after crystallization (eq 3). The

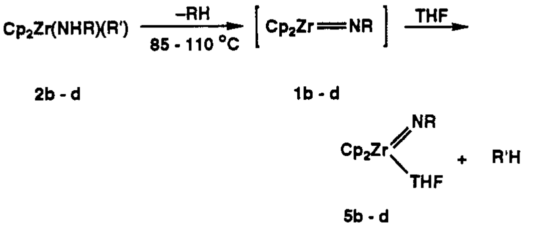

(3)

$^1$H and $^{13}$C{$^1$H} NMR resonances for the coordinated THF ligands in complexes **5b–d** were shifted relative to free THF. Resonances for the THF ligand of **5c** were broad at 25 °C ($^1$H NMR), suggesting that the cyclic ether is weakly bound to the zirconium center. When excess THF (2 equiv) was added to a benzene solution of **5c**, only one set of resonances for the free and bound THF was observed at 25 °C, indicating that bound and free THF exchange rapidly. This exchange was not observed at 25 °C on the $^1$H NMR time scale for complexes **5b** and **5d**.

In order to gain insight into the nature of the Zr—N linkage in Cp$_2$Zr(NR)(L) an X-ray diffraction study of **5b**

---

(12) Thorn, D. L.; Nugent, W. A.; Harlow, R. L. *J. Am. Chem. Soc.* **1981**, *103*, 357.

(13) Nugent, W. A.; Haymore, B. L. *Coord. Chem. Rev.* **1980**, *31*, 123.

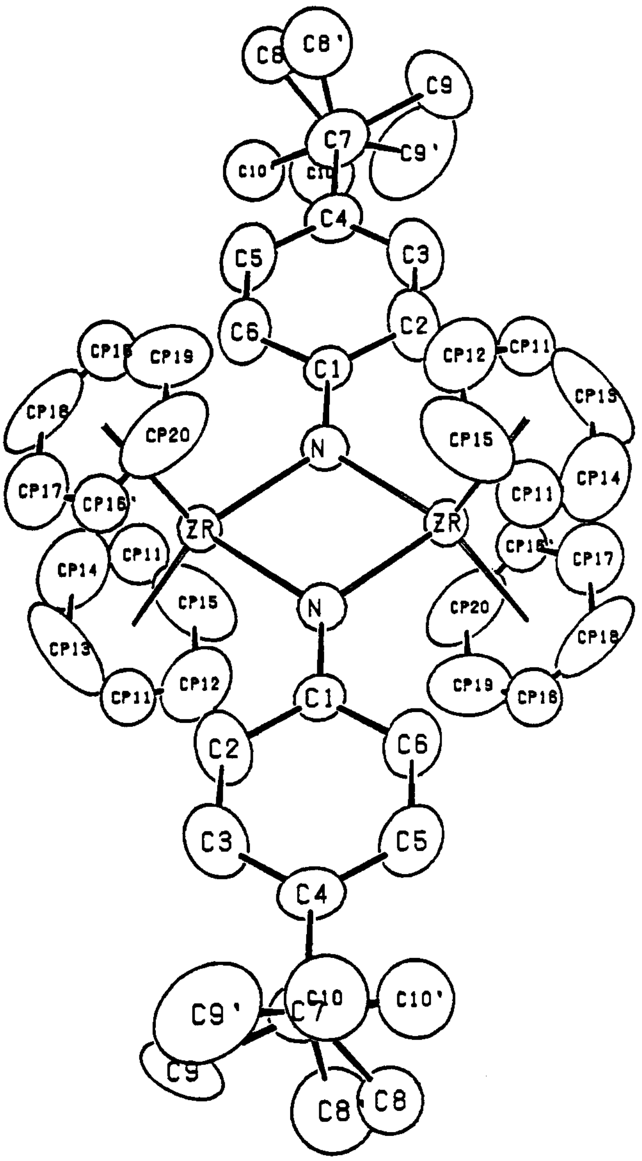

**Figure 1.** Geometry and labeling scheme for **4a**. The ellipsoids are scaled to represent the 50% probability surface.

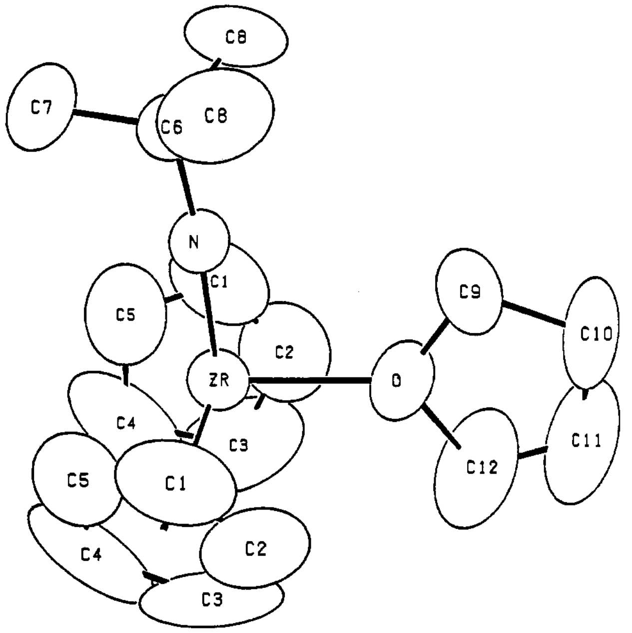

**Figure 2.** Geometry and labeling scheme for complex **5b**. The ellipsoids are scaled to represent the 50% probability surface.

**Table IV. Selected Intramolecular Distances (Å) and Esd's for Complex 5b**

| | | | |
|---|---|---|---|
| Zr–O | 2.240(4) | O–C9 | 1.414(8) |
| Zr–N | 1.826(4) | O–C12 | 1.485(9) |
| Zr–C1 | 2.579(6) | C9–C10 | 1.543(9) |
| Zr–C2 | 2.630(7) | C10–C11 | 1.424(14) |
| Zr–C3 | 2.666(6) | C11–C12 | 1.339(16) |
| Zr–C4 | 2.603(5) | C1–C2 | 1.277(10) |
| Zr–C5 | 2.540(5) | C1–C5 | 1.311(9) |
| Zr–CP | 2.325 | C2–C3 | 1.367(13) |
| N–C6 | 1.449(6) | C3–C4 | 1.533(12) |
| C6–C7 | 1.515(8) | C4–C5 | 1.408(10) |
| C6–C8 | 1.571(6) | | |

**Table V. Intramolecular Bond Angles (deg) and Esd's for Complex 5b**

| | | | |
|---|---|---|---|
| Cp–Zr–O | 102.17 | C9–O–C12 | 108.4(7) |
| Cp–Zr–N | 111.04 | O–C9–C10 | 103.9(6) |
| Cp–Zr–Cp | 128.84 | C9–C10–C11 | 107.8(7) |
| N–Zr–O | 94.53(16) | C10–C11–C12 | 109.5(8) |
| Zr–N–C6 | 174.4(3) | C11–C12–O | 110.3(10) |
| N–C6–C7 | 110.0(5) | C2–C1–C5 | 114.8(7) |
| N–C6–C8 | 108.7(3) | C1–C2–C3 | 109.6(8) |
| C7–C6–C8 | 110.4(3) | C2–C3–C4 | 104.8(7) |
| C8–C6–C8 | 108.5(6) | C3–C4–C5 | 102.2(6) |
| Zr–O–C9 | 124.3(4) | C1–C5–C4 | 108.4(7) |
| Zr–O–C12 | 127.3(6) | | |

was undertaken. Clear columnar crystals were grown from a toluene solution of the complex layered with hexanes at −30 °C; data collection conditions are outlined in Table I. The structure was solved in a manner similar to that of **4a**; bond lengths and bond angles are listed in Tables IV and V. An ORTEP diagram depicted in Figure 2 clearly shows the monomeric nature of **5b**. Like almost all terminal imido ligands[4] the Zr—N linkage is linear with a Zr—N—C bond angle of 174.4(3)° while the Zr—N bond length of 1.826 Å is ~0.2 Å shorter than those of Zr—N single bonds.[14] This complex can be compared to the monomeric $\eta^1$-hydrazido(2$^-$) complex Cp$_2$Zr(=NNPh$_2$)(DMAP)(DMAP = 4-(*N*,*N*-dimethylamino)pyridine) which exhibits a Zr=N bond distance of 1.873(7) Å and a Zr=N—N bond angle of 168.7(6)°.[15] The imido complexes ((2,6-$i$-Pr$_2$C$_6$H$_3$)HN)$_2$(py′)$_2$Zr=N(2,6-$i$-Pr$_2$C$_6$H$_3$) and ((2,6-$i$-Pr$_2$C$_6$H$_3$)O)$_2$(py′)$_2$Zr=N(2,6-$i$-Pr$_2$C$_6$H$_3$) (py′ = 4-pyrrolidinopyridine) (Figure 3) have recently been synthesized by Rothwell and co-workers.[3c] The Zr=N bond distances in these complexes were found to be 1.868(3) and 1.844(9) Å while the Zr—N—C$_{\text{ipso}}$ bond angles were 174.9(3) and 175.5(8)°, respectively.

Like those in **5c**, the THF ligands in the imido complexes **5b** and **d** are weakly bound and easily displaced. Thus, reaction of **5b** with triphenylphosphine oxide in benzene at 25 °C resulted in the rapid and quantitative ($^1$H NMR spectrometry) formation of the triphenylphosphine oxide adduct Cp$_2$Zr(NCMe$_3$)(OPPh$_3$), **6b** (eq 4), which can be crystallized in 92% yield from toluene layered with hexanes. A similar ligand exchange with triphenylphosphine sulfide was attempted; however the phosphine sulfide did not displace THF from **5b**. This difference in reactivity is consistent with the expected stronger binding of the "harder" oxygen atom to a zirconium(IV) center.

---

[14] The average bridging and terminal Zr–N distances in [(Me$_2$N)$_2$Zr($\mu$-NCMe$_3$)]$_2$ are 2.065(1) and 2.060(1) Å; see: Nugent, W. A.; Harlow, R. L. *Inorg. Chem.* **1979**, *18*, 2030. The Zr–N distances in the bis(pyrrolyl) compound Cp$_2$Zr(NC$_4$H$_4$)$_2$ are 2.167(2) and 2.171(2) Å; see: Bynum, R. V.; Hunter, W. E.; Rogers, R. D.; Atwood, J. T. *Inorg. Chem.* **1980**, *19*, 2368. The Zr–N bond distances of the amide ligands in complex A shown in Figure 3 are 2.134(4) and 2.150(3) Å; see ref 3c.

[15] Walsh, P. J.; Carney, M. J.; Bergman, R. G. *J. Am. Chem. Soc.* **1991**, *113*, 6343.

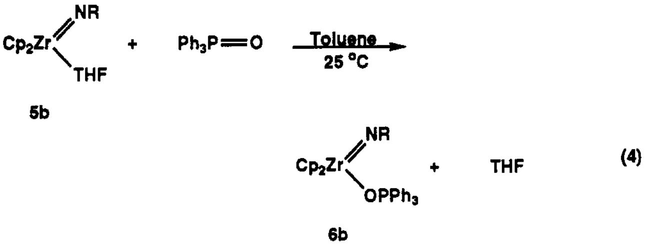

**Addition of C—H and N—H Bonds across the Zr=N Linkage.** In contrast to the formation of dimer **4a** from **2a**, thermolysis of the methyl amide **2b** in benzene (85 °C, 42 h) provided the phenyl amide $Cp_2Zr(NHCMe_3)(Ph)$, **7b** (eq 5), in 61% yield after recrystallization from toluene layered with hexanes at −30 °C. Methane was also produced in this reaction, as identified by $^1H$ NMR spectrometry. The proposed structure of **7b** is supported by $^1H$ and $^{13}C\{^1H\}$ NMR and IR spectrometry. The $^1H$ NMR spectrum of **7b** consists of resonances for the equivalent cyclopentadienyl ligands (5.73 ppm) and the *tert*-butyl (1.15 ppm) and phenyl groups (7.16–7.57 ppm), and a broad singlet (5.85 ppm) which integrated for one proton and was attributed to the N—H group of the amide ligand. The $^{13}C\{^1H\}$ NMR spectrum (THF-$d_8$) contained a resonance at 179 ppm, which falls in the range appropriate for the sp² hybridized carbon bound to the $Cp_2Zr$ center (170–190 ppm).[16] The IR spectrum of **7b** ($C_6H_6$) exhibited an N—H stretching absorption at 3299 cm$^{-1}$.

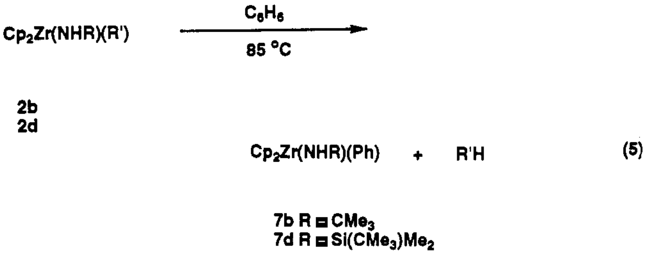

Similarly, the (dimethyl-*tert*-butylsilyl)amide **2d** reacted with benzene (28 h, 85 °C) to afford the phenyl amide $Cp_2Zr(NHSi(CMe_3)Me_2)(Ph)$ (**7d**) in 59% yield after recrystallization from toluene layered with hexanes at −30 °C. The spectroscopic properties of **7d** are similar to those of **7b**. The phenyl amide **7d** was independently synthesized by the room temperature addition of $H_2NSi(CMe_3)Me_2$ to the benzyne complex $Cp_2Zr(C_6H_4)(PMe_2Ph)$[17] in 89% yield, as determined by $^1H$ NMR integration against an internal standard (Scheme III). Thermolysis of the (2,6-dimethylphenyl)amide **2c** in benzene at 85 °C led to neohexane and cyclopentadienyl containing intractable products rather than the corresponding phenyl amide $Cp_2Zr(NH(2,6\text{-}Me_2C_6H_3))(Ph)$ (**7c**). The synthesis of **7c** was achieved using methodology developed by Erker,[18] Buchwald,[17] and their co-workers. They observed that heating a solution of $Cp_2ZrPh_2$ resulted in elimination of benzene with formation of the transient zirconium benzyne complex $Cp_2Zr(\eta^2\text{-}C_6H_4)$, as illustrated in Scheme III. This intermediate was trapped by unsaturated organic molecules to give insertion products and by Lewis bases to provide isolable benzyne complexes as their ligand adducts.[17,18] We found that this reactive intermediate can also be trapped by weakly acidic N—H protons of amines to furnish phenyl amide complexes $Cp_2Zr(NHR)(Ph)$, provided α-abstraction of benzene from the resulting phenyl amide complex is slow relative to formation of the benzyne complex. Thus, reaction of $Cp_2ZrPh_2$ with 2,6-dimethylaniline at 85 °C for 3 h (Scheme III) followed by recrystallization from a toluene solution by vapor phase diffusion of pentane at −30 °C provided **7c** in 63% isolated yield.

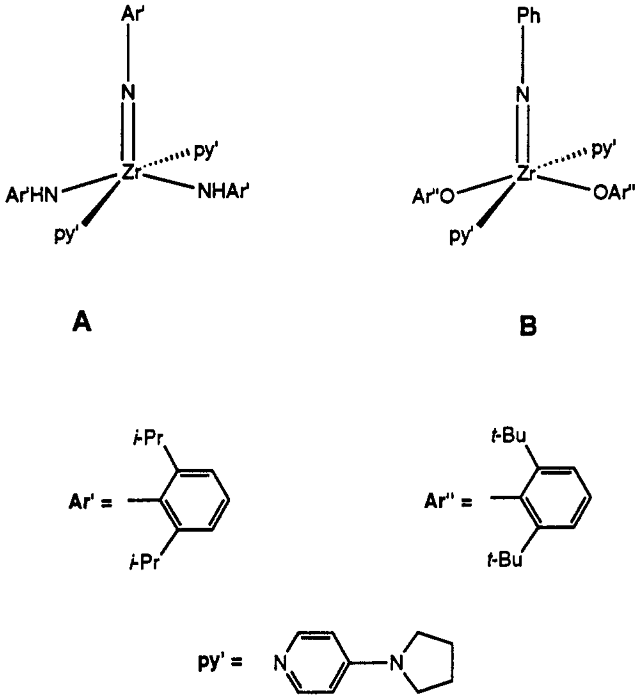

**Figure 3.** Illustration of the geometries of monomeric imido complexes A and B.

**Scheme III**

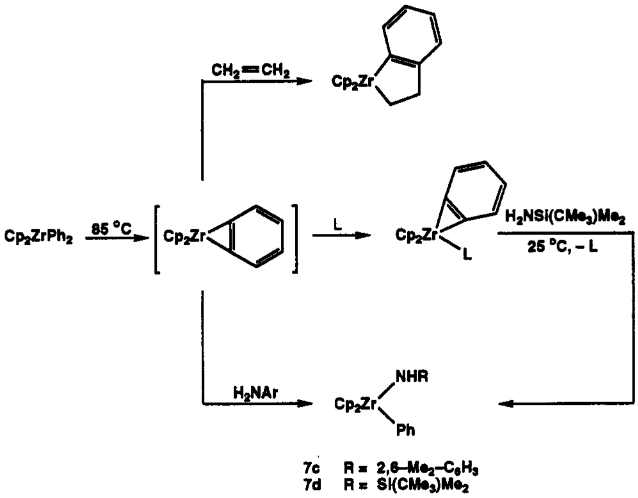

The monomeric imido complex **5b** can also be utilized to activate C–H bonds of benzene (eq 6). Heating a benzene solution of **5b** to 85 °C resulted in formation of free THF and phenyl amide complex **7b** in >95% yield by $^1H$ NMR spectrometry with a half-life of ~45 m. The monomeric imido complex **5c** also reacted with weakly acidic bonds. Addition of 2,6-dimethylaniline to a solution of **5c** at 25 °C resulted in the rapid formation of the bis-

---

[16] For example the $^{13}C$ resonance for the corresponding sp² hybridized carbon in $Cp^*_2ZrPh_2$ is 193.5 ppm; see: Schock, L. E.; Brock, C. P.; Marks, T. J. *Organometallics* **1987**, *6*, 232. In the metallacycle $Cp_2Zr(CPhCPhCHNSiMe_3)$ the sp² hybridized carbon resonates at 187.0 ppm; see: Buchwald, S. L.; Wannamaker, M. W.; Watson, B. T. *J. Am. Chem. Soc.* **1989**, *111*, 776.

[17] Buchwald, S. L.; Watson, B. T.; Huffman, J. C. *J. Am. Chem. Soc.* **1986**, *108*, 7411.

[18] Erker, G. *J. Organomet. Chem.* **1977**, *134*, 189 and references therein.

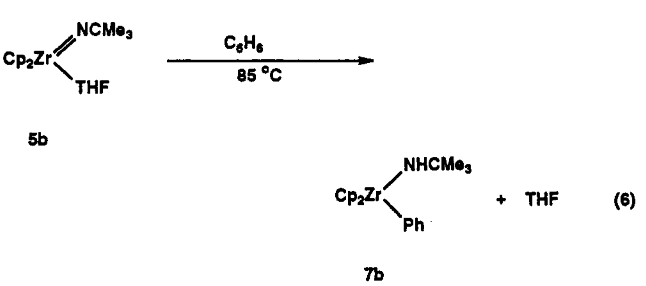

(amide) complex **3c** in >98% yield by $^1$H NMR spectrometry (eq 7).

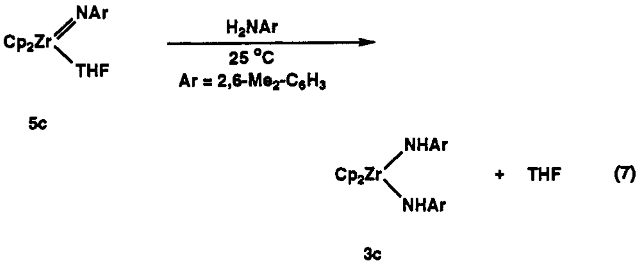

**Reactions of Cp$_2$Zr=NR with Alkynes and Olefins: Formation of Azametallacyclobutenes and Azametallacyclobutanes.** We have shown that heating the alkyl amide (**2a–d**) or the bis(amide) (**3b** and **3c**) complexes in the presence of internal alkynes leads to the formation of the azametallacyclobutenes, as illustrated in Scheme IV. Alkane R'H and enamine are also formed in these reactions. In a separate study[10] the mechanism of generation of enamine was found to involve an $\alpha$-abstraction of amine from the bis(amide) to generate the intermediate **1c** and free amine. This reactive intermediate undergoes a 2 + 2 cycloaddition with alkynes to provide azametallacyclobutenes.

Likewise, the addition of internal alkynes to the imido complexes **5b–d** also provided the metallacycles in high yield (eq 8). For example, addition of diphenylacetylene

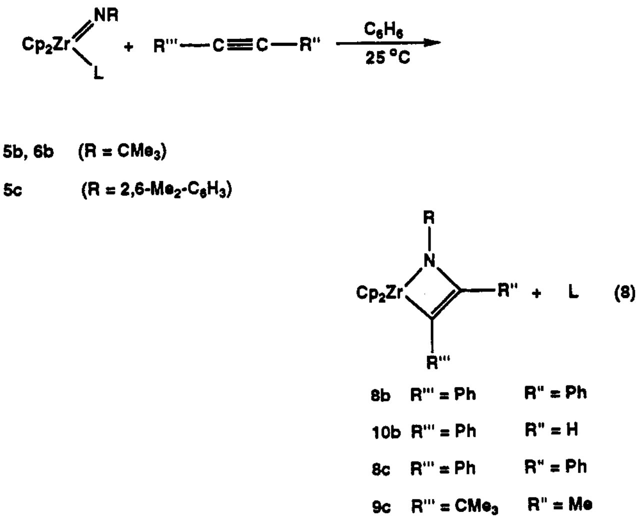

to a solution of the imido complex **5c** resulted in a rapid color change from yellow to brown with formation of the metallacycle **8c** in 97% yield, as determined by integration of the $^1$H NMR spectrum. Similar results were observed in the reaction of **5b** with diphenylacetylene to give **8b**. The imido complexes **5b–d** react rapidly under mild conditions (25 °C) and do not require the high temperatures (85–120 °C) used to generate the imido intermediates **1b–d** from the alkyl amide or bis(amide) complexes.

### Scheme IV

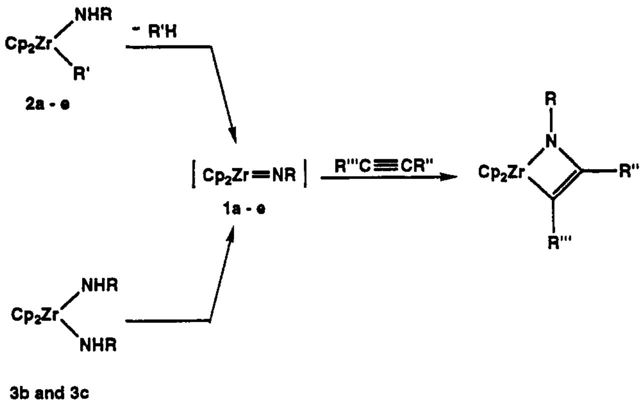

Reaction of the more robust Cp$_2$Zr(NCMe$_3$)(OPPh$_3$) (**6b**) with diphenylacetylene resulted in generation of metallacycle **8b** (eq 8). However, this conversion required a much longer reaction time (24 h compared to seconds for formation of **8b** from **5b** or formation of **8c** from **5c**). In addition, the facile generation of the imido intermediates **1b–d** from the THF adducts **5b–d** allows synthesis of compounds which are not available through thermolysis of the alkyl amides. For example, the reaction of the alkyl amide **2c** or bis(amide) **3c** with 4,4-dimethyl-2-pentyne at 85 °C led to intractable products, but by utilization of the imido complex **5c** at 25 °C this alkyne provided metallacycle **9c** (eq 8) in >98% yield, as determined by $^1$H NMR integration against an internal standard (70% isolated yield).[10b]

The imido complex **5b** also reacted with the terminal alkyne phenylacetylene to provide the metallacycle **10b** in 51% isolated yield (eq 8). Hydrolysis of **10b** with 5% HCl furnished phenylacetaldehyde which was identified by GCMS by comparison with an authentic sample.

The formation of the azametallacyclobutene is often reversible under the conditions (85–110 °C) required to generate the imido intermediates **1a–d** from the alkyl amides in the presence of internal alkynes.[10] When metallacycle **8c** (formed from PhCCPh) was heated to 95 °C with di-*p*-tolylacetylene, an equilibrium between the metallacycles **8c** and **11c** and the two diarylalkynes was observed by $^1$H NMR spectrometry (eq 9).[10] A similar

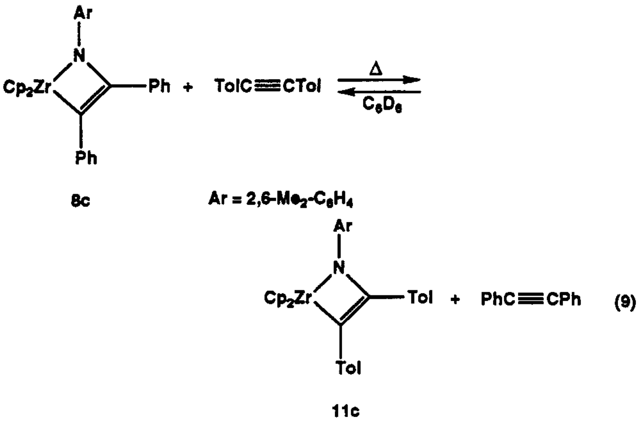

reversibility was observed in the reaction of the monomeric imido complexes **5b** and **5d** with olefins, but both the forward and the reverse reactions occur at room temperature. For example, reaction of the THF adduct **5b** with 3 equiv of norbornene resulted in equilibration ($K_{eq}$ = 0.3 at 25 °C, as determined by $^1$H NMR spectrometry) of the

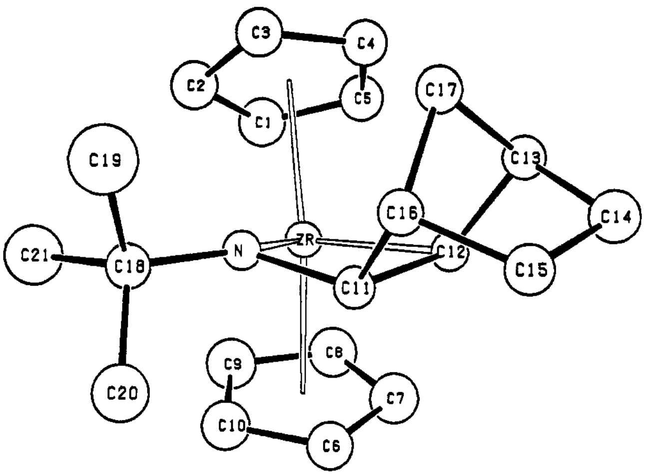

**Figure 4.** Geometry and labeling scheme for complex **12b**. The spheres are scaled to represent the 50% probability surface.

THF adduct **5b** and free norbornene with free THF and a new complex **12b** (eq 10). This material exhibits resonances in the $^{1}$H NMR spectra for two inequivalent cyclopentadienyl ligands (5.71 and 5.85 ppm), a new *tert*-butyl group, and a norbornene which no longer contains a plane of symmetry. This compound was prepared on a larger scale by adding an excess of norbornene (>30 equiv) to **5b** which resulted in essentially complete conversion to the metallacycle **12b**, as judged by $^{1}$H NMR spectrometry. The product was recrystallized from hexamethyldisiloxane albeit in low yield (46%) due to the high solubility of this material. The $^{13}$C{$^{1}$H} NMR spectrum ($C_6D_6$) contained resonances for the methine carbons (assigned by a DEPT NMR experiment[19]) at 40.33, 44.82, 45.42, and 75.37 ppm. The downfield shift of the 75.37 ppm resonance suggests that this signal is due to a carbon bound to nitrogen.[20]

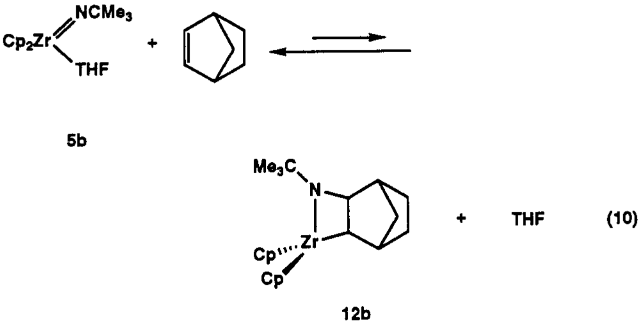

To verify the proposed connectivity of the metallacycle **12b**, single crystals were grown from hexamethyldisiloxane at −30 °C. X-ray diffraction data were collected at −95 °C, and a structure determination was carried out (Table I). The structure was solved in a fashion similar to that of **4a**; an ORTEP diagram is shown in Figure 4 with bond distances and angles listed in Tables VI and VII. From the ORTEP drawing it is clear that the imido intermediate **1b** has attacked the least hindered *exo* face of the norbornene double bond. Analogous stereoselectivity was observed with diborane which further extends the similarities in selectivity exhibited by these reagents.[21]

**Table VI. Selected Intramolecular Distances (Å) and Esd's for Complex 12b**

| | | | |
|---|---|---|---|
| Zr–N | 2.013(3) | C4–C5 | 1.429(5) |
| Zr–C11 | 2.578(3) | C6–C7 | 1.401(5) |
| Zr–C12 | 2.241(3) | C6–C10 | 1.396(5) |
| Zr–C1 | 2.559(4) | C7–C8 | 1.410(6) |
| Zr–C2 | 2.550(4) | C8–C9 | 1.410(5) |
| Zr–C3 | 2.575(4) | C9–C10 | 1.445(6) |
| Zr–C4 | 2.566(4) | C11–N | 1.488(4) |
| Zr–C5 | 2.571(4) | C18–N | 1.495(4) |
| Zr–Cp1 | 2.266 | C11–C12 | 1.623(4) |
| Zr–C6 | 2.553(4) | C11–C16 | 1.569(5) |
| Zr–C7 | 2.568(4) | C12–C13 | 1.529(5) |
| Zr–C8 | 2.597(4) | C13–C14 | 1.532(5) |
| Zr–C9 | 2.546(4) | C13–C17 | 1.554(5) |
| Zr–C10 | 2.551(4) | C14–C15 | 1.562(5) |
| Zr–Cp2 | 2.264 | C15–C16 | 1.551(5) |
| C1–C2 | 1.433(5) | C16–C17 | 1.578(5) |
| C1–C5 | 1.396(5) | C18–C19 | 1.538(6) |
| C2–C3 | 1.402(5) | C18–C20 | 1.513(5) |
| C3–C4 | 1.399(5) | C18–C21 | 1.555(5) |

**Table VII. Intramolecular Bond Angles (deg) and Esd's for Complex 12b**

| | | | |
|---|---|---|---|
| Cp1–Zr–N | 114.48 | C11–C16–C15 | 107.3(3) |
| Cp2–Zr–N | 113.05 | C11–C16–C17 | 101.7(3) |
| Cp1–Zr–C12 | 112.46 | C15–C16–C17 | 102.0(3) |
| Cp2–Zr–C12 | 103.95 | C13–C17–C16 | 93.2(3) |
| Cp1–Zr–Cp2 | 126.54 | N–C18–C19 | 111.2(3) |
| N–Zr–C12 | 72.37(11) | N–C18–C20 | 110.6(3) |
| Zr–N–C11 | 93.6(2) | N–C18–C21 | 106.1(3) |
| Zr–N–C18 | 143.6(2) | C19–C18–C20 | 113.5(3) |
| Zr–C12–C11 | 82.0(2) | C19–C18–C21 | 105.8(3) |
| Zr–C12–C13 | 131.2(2) | C20–C18–C21 | 109.4(3) |
| C11–N–C18 | 119.8(2) | C2–C1–C5 | 108.6(3) |
| N–C11–C12 | 108.0(2) | C1–C2–C3 | 106.4(3) |
| N–C11–C16 | 115.5(3) | C2–C3–C4 | 109.9(3) |
| C12–C11–C16 | 99.8(2) | C3–C4–C5 | 107.1(3) |
| C11–C12–C13 | 104.3(3) | C1–C5–C4 | 108.0(3) |
| C12–C13–C14 | 108.1(3) | C7–C6–C10 | 108.7(3) |
| C12–C13–C17 | 104.1(3) | C6–C7–C8 | 108.7(3) |
| C14–C13–C17 | 101.2(3) | C7–C8–C9 | 107.8(3) |
| C13–C14–C15 | 102.2(3) | C8–C9–C10 | 107.2(4) |
| C14–C15–C16 | 104.2(3) | C6–C10–C9 | 107.5(3) |

The Zr–N bond length of 2.013(3) Å is somewhat short,[14] while the Zr–C distance of 2.241(3) Å is typical of a single bond between these elements.[22] The N–C11 and C11–C12 distances of 1.488(4) and 1.623(4) Å are also indicative of single bonds.

Similar to the reaction of **5b** with norbornene, addition of ethylene to **5b** resulted in equilibration of the imido complex and ethylene with free THF and a new complex **13b** (Scheme V). The $^{1}$H NMR spectrum (Figure 5) of **13b** in toluene-$d_8$ at 10 °C consisted of singlets at 5.47, 1.94, and 0.96 ppm in a ratio of 10:4:9. The resonance at 1.94 ppm in the room temperature spectrum was assigned to a bound ethylene. The large separation of this resonance from that of free ethylene (5.25 ppm in toluene-$d_8$) demonstrated that exchange of bound ethylene for free ethylene was not occurring on the NMR time scale. As the sample was cooled in the probe of the NMR spectrometer the resonance assigned to the bound ethylene began to decoalesce, splitting into two multiplets (one of which moves into the resonance of the residual $C_6D_5$–$CD_2H$), as illustrated in Figure 6. In the $^{13}$C{$^{1}$H} NMR spectrum, we were unable to observe resonances for the bound ethylene at 25 °C; however, resonances attributed to this moiety were detected at −40 °C. At this temperature the two methylene resonances (assignedby a DEPT

---

[19] Derome, A. E. *Modern NMR Techniques for Chemistry Research*; Pergamon Press: Oxford, U.K., 1987; pp 143–151.

[20] Silverstein, R. M.; Bassler, G. C.; Morril, T. C. *Spectrometric Identification of Organic Compounds*; John Wiley & Sons: New York, 1981; p 258–272.

[21] Brown, H. C.; Kawakami, J. H.; Liu, K. T. *J. Am. Chem. Soc.* **1973**, *95*, 2209.

[22] Cardin, D. J.; Lappert, M. F.; Raston, C. L. *Chemistry of Organo-Zirconium and -Hafrium Compounds*; Ellis Horwood Limited: New York, 1986; pp 68–75.

**Table VIII. $^1$H NMR Spectroscopic Data**

| compd | δ (ppm) | mult | *J* (Hz) | area | assgnt |
|---|---|---|---|---|---|
| **2a**$^a$ | 0.30 | s | | 3 | C$H_3$ |
| | 1.32 | s | | 9 | C(C$H_3$)$_3$ |
| | 5.65 | s | | 10 | C$_5H_5$ |
| | 6.55 | s | | 1 | N–*H* |
| | 6.73 | d | 8.48 | 2 | aromatic C–*H* |
| | 7.25 | d | 8.48 | 2 | aromatic C–*H* |
| **2b**$^a$ | 0.11 | s | | 3 | C$H_3$ |
| | 1.10 | s | | 9 | C(C$H_3$)$_3$ |
| | 5.28 | s | | 1 | N–*H* |
| | 5.69 | s | | 10 | C$_5H_5$ |
| **2c**$^a$ | 0.78 | m | | 2 | C$H_2$ |
| | 1.09 | s | | 9 | C(C$H_3$) |
| | 1.54 | m | | 2 | C$H_2$ |
| | 2.08 | s | | 6 | C$H_3$ |
| | 5.54 | s | | 10 | C$_5H_5$ |
| | 5.73 | s | | 1 | N–*H* |
| | 6.93 | t | 7.44 | 1 | aromatic C–*H* |
| | 7.09 | d | 7.44 | 2 | aromatic C–*H* |
| **2d**$^a$ | 0.15 | s | | 6 | Si(C$H_3$)$_2$ |
| | 0.75 | m | | 2 | C$H_2$ |
| | 1.04 | s | | 9 | C(C$H_3$)$_3$ |
| | 1.48 | s | | 9 | C(C$H_3$)$_3$ |
| | 1.50 | m | | 2 | C$H_2$ |
| | 4.43 | s | | 1 | N–*H* |
| | 5.72 | s | | 10 | C$_5H_5$ |
| **2e**$^a$ | 0.65 | m | | 2 | C$H_2$ |
| | 1.00 | s | | 9 | C(C$H_3$)$_3$ |
| | 1.34 | m | | 2 | C$H_2$ |
| | 5.37 | d | 12.41 | 1 | N*H* |
| | 5.55 | s | | 10 | C$_5H_5$ |
| | 5.64 | d | 12.41 | 1 | C*H*Ph$_2$ |
| | 7.02 | tt | 6.64, 2.20 | 2 | aromatic C–*H* |
| | 7.13 | m | | 8 | aromatic C–*H* |
| **3a**$^b$ | 1.22 | s | | 18 | C(C$H_3$)$_3$ |
| | 6.14 | s | | 10 | C$_5H_5$ |
| | 6.48 | s | | 2 | N–*H* |
| | 6.56 | d | 8.53 | 4 | aromatic C–*H* |
| | 7.00 | d | 8.53 | 4 | aromatic C–*H* |
| **3b**$^a$ | 1.24 | s | | 18 | C(C$H_3$)$_3$ |
| | 3.77 | s | | 2 | N–*H* |
| | 5.83 | s | | 10 | C$_5H_5$ |
| **3c**$^b$ | 2.32 | s | | 12 | C$H_3$ |
| | 5.85 | s | | 2 | N–*H* |
| | 5.96 | s | | 10 | C$_5H_5$ |
| | 6.63 | t | 7.40 | 2 | aromatic C–*H* |
| | 6.93 | d | 7.40 | 4 | aromatic C–*H* |
| **3d**$^a$ | 0.19 | s | | 12 | C$H_3$ |
| | 0.98 | s | | 18 | C(C$H_3$)$_3$ |
| | 2.90 | s | | 2 | N–*H* |
| | 5.86 | s | | 10 | C$_5H_5$ |
| **4a**$^c$ | 1.37 | s | | 9 | C(C$H_3$)$_3$ |
| | 6.02 | d | 8.56 | 2 | aromatic C–*H* |
| | 6.66 | s | | 10 | C$_5H_5$ |
| | 7.27 | d | 8.50 | 2 | aromatic C–*H* |
| **5b**$^a$ | 1.06 | m | | 4 | C$H_2$ |
| | 1.28 | s | | 9 | C(C$H_3$)$_3$ |
| | 3.36 | m | | 4 | C$H_2$ |
| | 6.10 | s | | 10 | C$_5H_5$ |
| **5c**$^a$ | 1.06 | m | | 4 | C$H_2$ |
| | 2.36 | s | | 6 | C$H_3$ |
| | 3.29 | m | | 4 | C$H_2$ |
| | 5.97 | s | | 10 | C$_5H_5$ |
| | 6.72 | t | 7.30 | 1 | aromatic C–*H* |
| | 7.24 | d | 7.30 | 2 | aromatic C–*H* |
| **5d**$^a$ | 0.22 | s | | 6 | C$H_3$ |
| | 1.04 | m | | 4 | C$H_2$ |
| | 1.22 | s | | 9 | C(C$H_3$)$_3$ |
| | 3.31 | m | | 4 | C$H_2$ |
| | 6.05 | s | | 10 | C$_5H_5$ |
| **6b**$^a$ | 1.28 | s | | 9 | C(C$H_3$)$_3$ |
| | 6.27 | s | | 10 | C5$H_5$ |
| | 7.02 | m | | 9 | aromatic C–*H* |
| | 7.67 | dd | 8.01, 4.69 | 6 | aromatic C–*H* |
| **7b**$^a$ | 1.15 | s | | 9 | C(C$H_3$)$_3$ |
| | 5.73 | s | | 10 | C$_5H_5$ |
| | 5.85 | s | | 1 | N–*H* |
| | 7.16 | m | | 1 | aromatic C–*H* |
| | 7.28 | m | | 2 | aromatic C–*H* |
| | 7.57 | m | | 2 | aromatic C–*H* |
| **7c**$^a$ | 2.01 | s | | 6 | C$H_3$ |
| | 5.61 | s | | 10 | C$_5H_5$ |
| | 6.29 | s | | 1 | N–*H* |
| | 6.90 | t | 7.45 | 1 | aromatic C–*H* |
| | 7.05 | d | 7.40 | 2 | aromatic C–*H* |
| | 7.19 | tt | 7.54, 1.44 | 1 | aromatic C–*H* |
| | 7.28 | t | 7.49 | 2 | aromatic C–*H* |
| | 7.57 | dd | 7.83, 1.34 | 2 | aromatic C–*H* |
| **7d**$^a$ | 0.11 | s | | 6 | C$H_3$ |
| | 0.94 | s | | 9 | C(C$H_3$)$_3$ |
| | 5.24 | s | | 1 | N–*H* |
| | 5.77 | s | | 10 | C$_5H_5$ |
| | 7.13 | t | 8.28 | 1 | aromatic C-*H* |
| | 7.24 | td | 7.41, 1.20 | 2 | aromatic C–*H* |
| | 7.43 | dd | 7.54, 1.11 | 2 | aromtic C–*H* |
| **10b**$^a$ | 1.04 | s | | 9 | C(C$H_3$)$_3$ |
| | 5.79 | s | | 10 | C$_5H_5$ |
| | 7.12 | t | 7.25 | 1 | aromatic C–*H* |
| | 7.27 | dd | 7.16, 0.53 | 2 | aromatic C–*H* |
| | 7.36 | dd | 7.16, 0.53 | 2 | aromatic C–*H* |
| | 7.37 | t | 7.65 | 2 | aromatic C–*H* |
| **12b**$^a$ | 0.93 | dt | 9.20, 1.30 | 1 | C–*H* |
| | 1.06 | s | | 9 | C(C$H_3$)$_3$ |
| | 1.18 | m | | 1 | C–*H* |
| | 1.32 | m | | 1 | C–*H* |
| | 1.41 | d | 9.02 | 1 | C–*H* |
| | 1.68 | m | | 2 | C–*H* |
| | 1.91 | d | 5.86 | 1 | C–*H* |
| | 2.04 | s | | 1 | C–*H* |
| | 2.57 | 2 | | 1 | C–*H* |
| | 2.64 | d | 5.29 | 1 | C–*H* |
| | 5.71 | s | | 5 | C$_5H_5$ |
| | 5.85 | s | | 5 | C$_5H_5$ |
| **13b**$^b$ | 0.96 | s | | 9 | C(C$H_3$)$_3$ |
| | 1.94 | s | | 4 | C$H_2$ |
| | 5.47 | s | | 10 | C$_5H_5$ |
| **16**$^b$ | 1.17 | s | | 9 | C(C$H_3$)$_3$ |
| | 1.27 | s | | 9 | C(C$H_3$)$_3$ |
| | 1.64 | s | | 9 | C(C$H_3$)$_3$ |
| | 5.67 | s | | 10 | C$_5$H$_5$ |
| **17**$^a$ | 1.21 | s | | 9 | C(C$H_3$)$_3$ |
| | 1.64 | s | | 3 | C$H_3$ |
| | 3.98 | s | | 1 | N–*H* |
| | 4.25 | s (br) | | 2 | C$H_2$ |
| | 4.86 | m | | 1 | C*H* |
| | 5.09 | m | | 1 | C*H* |
| | 5.96 | s | | 10 | C$_5H_5$ |
| **19e**$^a$ | 5.45 | s | | 1 | C*H*Ph$_2$ |
| | 5.83 | s | | 10 | C$_5H_5$ |
| | 6.79 | dd | 8.41, 1.25 | 2 | aromatic C–*H* |
| | 6.91 | tt | 7.27, 1.23 | 1 | aromatic C–*H* |
| | 7.10 | m | | 17 | aromatic C–*H* |

$^a$ $C_6D_6$. $^b$ THF-$d_8$. $^c$ Pyridine-$d_5$. $^d$ $CD_2Cl_2$.

NMR experiment) were observed at 25.8 and 39.7 ppm. The low temperature $^{13}C\{^1H\}$ NMR spectrum of **13b** exhibits similarities to that of the azametallacyclobutane formed from norbornene and **5b**, the resonance at 39.7 ppm assigned to the carbon bound to nitrogen.

**Reaction of $Cp_2Zr{=}NCMe_3$ with Benzophenone and with *tert*-Butyl Isocyanate.** Monomer **5b** was found to react with organic carbonyl compounds, as illustrated in Scheme VI. When the imido complex **5b** was treated with benzophenone, a white precipitate formed (presumably polymeric zirconocene oxides) as well as metathesis product, the *tert*-butylimine of benzophenone (**14**), in 89% yield, as determined by $^1$H NMR integration against an internal standard. Analogous reactivity was observed in the reaction of **5b** with *tert*-butyl isocyanate which provided 1,3-di-*tert*-butylcarbodiimide (**15**) (65%

Table IX. $^{13}$C($^1$H) NMR Spectroscopic Data$^a$

| compd | δ (ppm) | assgnt | compd | δ (ppm) | assgnt | compd | δ (ppm) | assgnt |
|---|---|---|---|---|---|---|---|---|
| **2a**$^b$ | 20.32 | $\mathit{C}\mathrm{H}_3$ | **4a**$^d$ | 32.00 | $\mathrm{C}(\mathit{C}\mathrm{H}_3)_3$ | **10b**$^c$ | 31.88 | $\mathrm{C}(\mathit{C}\mathrm{H}_3)_3$ |
|  | 32.02 | $\mathrm{C}(\mathit{C}\mathrm{H}_3)_3$ |  | 34.15 | $\mathit{C}(\mathrm{CH}_3)_3$ |  | 55.37 | $\mathit{C}(\mathrm{CH}_3)_3$ |
|  | 34.48 | $\mathit{C}(\mathrm{CH}_3)_3$ |  | 113.13 | $\mathit{C}_5\mathrm{H}_5$ |  | 110.31 | $\mathit{C}_5\mathrm{H}_5$ |
|  | 110.54 | $\mathit{C}_5\mathrm{H}_5$ |  | 120.42 | aromatic *C*–H |  | 122.84 | *C*–H |
|  | 119.94 | aromatic *C*–H |  | 124.90 | aromatic *C*–H |  | 125.07 | *C*–H |
|  | 125.45 | aromatic *C*–H |  | 139.39 | quat |  | 128.19 | *C*–H |
|  | 141.51 | quat |  | 156.01 | quat |  | 128.24 | *C*–H |
|  | 154.69 | quat | **5b**$^c$ | 25.81 | $\mathit{C}\mathrm{H}_2$ |  | 146.61 | quat |
| **2b**$^c$ | 15.89 | $\mathit{C}\mathrm{H}_3$ |  | 34.46 | $\mathrm{C}(\mathit{C}\mathrm{H}_3)_3$ |  | 165.93 | quat |
|  | 34.46 | $\mathrm{C}(\mathit{C}\mathrm{H}_3)_3$ |  | 62.09 | $\mathit{C}(\mathrm{CH}_3)_3$ | **12b**$^c$ | 26.64 | $\mathit{C}\mathrm{H}_2$ |
|  | 56.50 | $\mathit{C}(\mathrm{CH}_3)_3$ |  | 77.64 | $\mathit{C}\mathrm{H}_2$ |  | 32.20 | $\mathrm{C}(\mathit{C}\mathrm{H}_3)_3$ |
|  | 108.99 | $\mathit{C}_5\mathrm{H}_5$ |  | 108.85 | $\mathit{C}_5\mathrm{H}_5$ |  | 33.40 | $\mathit{C}\mathrm{H}_2$ |
| **2c**$^c$ | 20.34 | $\mathit{C}\mathrm{H}_3$ | **5c**$^c$ | 21.04 | $\mathit{C}\mathrm{H}_2$ |  | 36.02 | $\mathit{C}\mathrm{H}_2$ |
|  | 29.48 | $\mathrm{C}(\mathit{C}\mathrm{H}_3)_3$ |  | 25.37 | $\mathit{C}\mathrm{H}_3$ |  | 40.33 | $\mathit{C}\mathrm{H}$ |
|  | 33.09 | $\mathit{C}\mathrm{H}_2$ |  | 77.00 | $\mathit{C}\mathrm{H}_2$ |  | 44.82 | $\mathit{C}\mathrm{H}$ |
|  | 34.32 | $\mathit{C}\mathrm{H}_2$ |  | 110.43 | $\mathit{C}_5\mathrm{H}_5$ |  | 45.42 | $\mathit{C}\mathrm{H}$ |
|  | 48.94 | $\mathit{C}(\mathrm{CH}_3)_3$ |  | 115.15 | quat |  | 56.12 | $\mathit{C}(\mathrm{CH}_3)_3$ |
|  | 109.92 | $\mathit{C}_5\mathrm{H}_5$ |  | 125.37 | aromatic *C*–H |  | 75.37 | $\mathit{C}\mathrm{H}$ |
|  | 122.40 | aromatic *C*–H |  | 127.93 | aromatic *C*–H |  | 109.55 | $\mathit{C}_5\mathrm{H}_5$ |
|  | 128.20 | aromatic *C*–H |  | 159.80 | quat |  | 110.09 | $\mathit{C}_5\mathrm{H}_5$ |
|  | 131.08 | quat | **5d**$^c$ | −0.56 | $\mathit{C}\mathrm{H}_3$ | **13b**$^e$ | 25.82 | $\mathit{C}\mathrm{H}_2$ |
|  | 155.39 | quat |  | 19.33 | $\mathrm{C}(\mathit{C}\mathrm{H}_3)_3$ |  | 30.17 | $\mathrm{C}(\mathit{C}\mathrm{H}_3)_3$ |
| **2d**$^c$ | −1.40 | $\mathit{C}\mathrm{H}_3$ |  | 25.72 | $\mathit{C}\mathrm{H}_2$ |  | 39.73 | $\mathit{C}\mathrm{H}_2$ |
|  | 18.78 | $\mathit{C}(\mathrm{CH}_3)_3$ |  | 27.63 | $\mathit{C}(\mathrm{CH}_3)_3$ |  | 55.67 | $\mathit{C}(\mathrm{CH}_3)_3$ |
|  | 26.72 | $\mathrm{C}(\mathit{C}\mathrm{H}_3)_3$ |  | 77.67 | $\mathit{C}\mathrm{H}_2$ |  | 109.81 | $\mathit{C}_5\mathrm{H}_5$ |
|  | 29.39 | $\mathrm{C}(\mathit{C}\mathrm{H}_3)_3$ |  | 109.91 | $\mathit{C}_5\mathrm{H}_5$ | **16**$^b$ | 28.63 | $\mathrm{C}(\mathit{C}\mathrm{H}_3)_3$ |
|  | 33.14 | $\mathit{C}(\mathrm{CH}_3)_3$ | **6b**$^c$ | 34.25 | $\mathrm{C}(\mathit{C}\mathrm{H}_3)_3$ |  | 29.59 | $\mathrm{C}(\mathit{C}\mathrm{H}_3)_3$ |
|  | 34.28 | $\mathit{C}\mathrm{H}_2$ |  | 61.12 | $\mathit{C}(\mathrm{CH}_3)_3$ |  | 33.82 | $\mathrm{C}(\mathit{C}\mathrm{H}_3)_3$ |
|  | 49.56 | $\mathit{C}\mathrm{H}_2$ |  | 108.81 | $\mathit{C}_5\mathrm{H}_5$ |  | 55.41 | $\mathit{C}(\mathrm{CH}_3)_3$ |
|  | 109.77 | $\mathit{C}_5\mathrm{H}_5$ |  | 128.78$^f$ | aromatic *C*–H |  | 56.17 | $\mathit{C}(\mathrm{CH}_3)_3$ |
| **2e**$^c$ | 29.41 | $\mathrm{C}(\mathit{C}\mathrm{H}_3)_3$ |  | 128.97$^g$ | quat |  | 58.69 | $\mathit{C}(\mathrm{CH}_3)_3$ |
|  | 32.13 | $\mathit{C}\mathrm{H}_2$ |  | 132.89$^h$ | aromatic *C*–H |  | 105.48 | $\mathit{C}_5\mathrm{H}_5$ |
|  | 33.05 | $\mathit{C}\mathrm{H}_2$ |  | 133.16$^i$ | aromatic *C*–H |  | 155.07$^j$ | $\mathit{C}\mathrm{N}^t\mathrm{Bu}$ |
|  | 48.66 | $\mathit{C}(\mathrm{CH}_3)_3$ | **7b**$^b$ | 34.69 | $\mathrm{C}(\mathit{C}\mathrm{H}_3)_3$ |  | 176.14 | $\mathrm{N}\mathit{C}\mathrm{N}$ |
|  | 71.51 | $\mathit{C}\mathrm{HPh}_2$ |  | 58.61 | $\mathit{C}(\mathrm{CH}_3)_3$ | **17**$^c$ | 19.16 | $\mathit{C}\mathrm{H}_3$ |
|  | 109.26 | $\mathit{C}_5\mathrm{H}_5$ |  | 110.36 | $\mathit{C}_5\mathrm{H}_5$ |  | 34.66 | $\mathrm{C}(\mathit{C}\mathrm{H}_3)_3$ |
|  | 126.58 | aromatic *C*–H |  | 123.84 | aromatic *C*–H |  | 55.59 | $\mathit{C}(\mathrm{CH}_3)_3$ |
|  | 127.49 | aromatic *C*–H |  | 126.45 | aromatic *C*–H |  | 77.26 | $\mathrm{C}\mathit{H}_2$ |
|  | 128.45 | aromatic *C*–H |  | 142.04 | aromatic *C*–H |  | 108.11 | $\mathrm{C}\mathit{H}_2$ |
|  | 149.31 | quat |  | 179.13 | quat |  | 111.07 | $\mathit{C}_5\mathrm{H}_5$ |
| **3a**$^b$ | 32.07 | $\mathrm{C}(\mathit{CH}_3)_3$ | **7c**$^c$ | 21.15 | $\mathit{C}\mathrm{H}_3$ |  | 147.22 | quat |
|  | 34.37 | $\mathit{C}(\mathrm{CH}_3)_3$ |  | 110.83 | $\mathit{C}_5\mathrm{H}_5$ | **19e**$^b$ | 68.57 | *C*–H |
|  | 111.15 | $\mathit{C}_5\mathrm{H}_5$ |  | 122.69 | aromatic *C*–H |  | 112.08 | $\mathit{C}_5\mathrm{H}_5$ |
|  | 118.66 | aromatic *C*–H |  | 124.58 | aromatic *C*–H |  | 121.89 | aromatic *C*–H |
|  | 125.38 | aromatic *C*–H |  | 126.73 | aromatic *C*–H |  | 127.01 | aromatic *C*–H |
|  | 139.67 | quat |  | 128.33 | aromatic *C*–H |  | 127.23 | aromatic *C*–H |
|  | 154.75 | quat |  | 131.09 | quat |  | 127.75 | aromatic *C*–H |
| **3b**$^c$ | 34.45 | $\mathrm{C}(\mathit{C}\mathrm{H}_3)_3$ |  | 140.76 | aromatic *C*–H |  | 127.84 | aromatic *C*–H |
|  | 55.20 | $\mathit{C}(\mathrm{CH}_3)_3$ |  | 155.74 | quat |  | 128.48 | aromatic *C*–H |
|  | 110.12 | $\mathit{C}_5\mathrm{H}_5$ |  | 179.00 | quat |  | 128.63 | aromatic *C*–H |
| **3c**$^b$ | 20.76 | $\mathit{C}\mathrm{H}_3$ | **7d**$^c$ | −1.17 | $\mathit{C}\mathrm{H}_3$ |  | 129.03 | aromatic *C*–H |
|  | 112.12 | $\mathit{C}_5\mathrm{H}_5$ |  | 18.68 | $\mathrm{C}(\mathit{C}\mathrm{H}_3)_3$ |  | 129.64 | quat |
|  | 120.50 | aromatic *C*–H |  | 26.70 | $\mathit{C}(\mathrm{CH}_3)_3$ |  | 130.28 | aromatic *C*–H |
|  | 128.51 | aromatic *C*–H |  | 110.62 | $\mathit{C}_5\mathrm{H}_5$ |  | 136.25 | quat |
|  | 129.82 | quat |  | 124.43 | aromatic *C*–H |  | 147.17 | quat |
|  | 157.92 | quat |  | 126.86 | aromatic *C*–H |  | 149.07 | quat |
| **3d**$^c$ | −1.21 | $\mathit{C}\mathrm{H}_3$ |  | 140.59 | aromatic *C*–H |  | 163.14 | quat |
|  | 19.15 | $\mathit{C}(\mathrm{CH}_3)_3$ |  | 179.11 | quat |  |  |  |
|  | 27.00 | $\mathrm{C}(\mathit{C}\mathrm{H}_3)_3$ |  |  |  |  |  |  |
|  | 111.19 | $\mathit{C}_5\mathrm{H}_5$ |  |  |  |  |  |  |

[a] All resonances are singlets unless otherwise noted. [b] THF-$d_8$, 25 °C. [c] $C_6D_6$, 25 °C. [d] Pyridine-$d_5$, 25 °C. [e] Toluene-$d_8$, −41 °C. [f] d, $J$ = 12.89 Hz. [g] d, $J$ = 109.66 Hz. [h] d, $J$ = 10.72 Hz. [i] $J$ = 2.06 Hz. [j] t, $J$ = 12.60 Hz.

by $^1$H NMR spectrometry). These compounds were also identified by GCMS.

**Reaction of $Cp_2Zr{=}NCMe_3$ with *tert*-Butyl Isocyanide and Isobutylene Oxide.** Compound **5b** was also found to react with 2 equiv of *tert*-butyl isocyanide, as shown in Scheme VII. The $^1$H NMR spectrum (THF-$d_8$) of the new compound **16** consisted of four singlets at 1.17, 1.27, 1.64, and 5.67 ppm in a ratio of 9:9:9:10, while the $^{13}$C{$^1$H} NMR spectrum (THF-$d_8$) contained resonances for the three inequivalent *tert*-butyl groups, the cyclopentadienyl ligands, a triplet at 155 ppm ($J(^{13}\mathrm{C}—^{14}\mathrm{N})$ = 13 Hz assigned to a terminal isonitrile[23]) and a singlet at 176 ppm. The IR spectrum of **16** (THF) exhibits strong absorptions at 2186 and 1570 cm$^{-1}$. These data support the structure of **16** as the $\eta^2$-1,3-di-*tert*-butylcarbodiimide isocyanide complex (Scheme VII). Reaction of $Cp_2Zr(NCMe_3)(OPPh_3)$ with *tert*-butyl isocyanide also led to rapid formation of **16** ($^1$H NMR spectrometry). Attempts to induce the $\eta^2$-1,3-di-*tert*-butylcarbodiimide complex to react with alkynes were unsuccessful.

---

[23] Compounds with axial symmetric electron density at the nitrogen nucleus frequently show similar coupling.

**Scheme V**

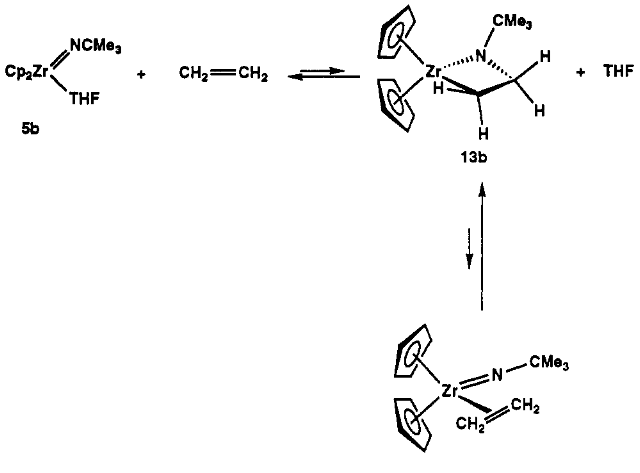

The imido complex **5b** was also found to attack epoxides, leading to ring-opened products containing strong zirconium–oxygen $\sigma$ bonds. Thus, addition of isobutylene oxide to **5b** resulted in formation of complex 17 (Scheme VIII). Attempts to purify this material completely by crystallization led to decomposition. However, its structure could be assigned with reasonable confidence by NMR and IR spectrometry. The $^1$H NMR spectrum of 17 ($C_6D_6$) contained singlets for the two equivalent cyclopentadienyl ligands (5.93 ppm), the *tert*-butyl group (1.23 ppm), a methyl group (1.66 ppm), and a methylene group (4.28 ppm) in a ratio of 10:9:3:2 by integration. The spectrum also contained three additional resonances integrating to a single proton each. A broad singlet characteristic of an N–H proton was observed at 3.98 ppm, while multiplets at 4.90 and 5.13 ppm with small complex coupling patterns were assigned to the geminal protons of an unsymmetrically substituted terminal olefin. The $^{13}C\{^1H\}$ NMR spectrum contained resonances assigned to the methylenes by a DEPT NMR experiment at 77.26 and 108.11 ppm, the latter located at the terminus of the double bond. The IR stretching absorptions observed at 3338 and 1654 cm$^{-1}$ were attributed to the amide N–H proton and the C–C double bond.

**$\alpha$- vs $\beta$-Abstraction: Preference for Formation of the Imido or $\eta^2$-Imine Complexes.** In separate systems, both $\alpha$- and $\beta$-abstraction have been observed for zirconocene alkylamides, leading to imido $Cp_2Zr{=}NR$ (1) and $\eta^2$-imine (or azametallacyclopropane) $Cp_2Zr(NR{-}CHR)$ (18) intermediates, respectively (Scheme IX). However, amides which contain both $\alpha$-N—H and $\beta$-C—H bonds have not been examined. With this in mind the *tert*-butyldimethylene amide $Cp_2Zr(NHCHPh_2)(CH_2CH_2CMe_3)$ (**2e**) was prepared using procedures similar to those described above. Heating **2e** with diphenylacetylene to 115 °C for 24 h afforded the green azametallacyclobutene complex **19e** in 64% yield (Scheme X). Formation of **19e** indicates that in the alkylamide **2e** $\alpha$-extrusion predominates over $\beta$-extrusion.

## Discussion

**Synthesis of Bis(amides) and Mechanism of Their Formation.** Zirconium bis(amides) of the general structure $Cp_2Zr(NHR)_2$ have been prepared by two complementary methodologies. The traditional route, room temperature displacement of chloride from $Cp_2ZrCl_2$ by a lithium amide, proved to be successful for the synthesis of bis(amides) **3a** and **3c** (eq 2). Reaction of 2 equiv of $LiNHCMe_3$ or $LiNHSi(CMe_3)Me_2$ with $Cp_2ZrCl_2$ did not lead to the formation of **3b** or **3d** but instead led to intractable products. Alternatively, the reaction of $Cp_2ZrMe_2$ with amine at elevated temperatures (85 °C for **3a**, 140 °C for **3b–d**) provided the bis(amide) complexes (Scheme I).

The wide variation in temperature required to synthesize the bis(amides) via $Cp_2ZrMe_2$ suggests that the first step of the reaction involves both the amine and $Cp_2ZrMe_2$. This experimental observation along with the coordinatively unsaturated nature of the zirconium center and the relatively high p$K_a$ of amines leads us to suggest that the mechanism of formation of the bis(amides) from $Cp_2ZrMe_2$ most likely involves initial coordination of the amine to the 16 electron zirconium center followed by proton transfer to form the methyl amide complex $Cp_2Zr(NHR)(Me)$ and methane (Scheme I). In the formation of the bis(amide) **3a** the methyl amide **2a** was observed as an intermediate when the reaction was monitored by $^1$H NMR spectrometry. Methyl amides were also assumed to be intermediates in the formation of **3b–d** but could not be detected.

Heating alkyl amides **2a–c** in the presence of the corresponding amines results in the formation of the bis(amides) **3a–c**. The kinetics of the thermolysis of the methyl amide **2a** in the presence of 1.87, 3.97, and 5.58 equiv of 4-*tert*-butylaniline gave rate constants of 4.97, 5.10, and $4.76 \times 10^{-5}$ s$^{-1}$, demonstrating that the rate is independent of the concentration of amine. This is inconsistent with a bimolecular pathway involving coordination of the amine and protonation of the remaining methyl group of the methyl amides. It instead supports a pathway involving unimolecular $\alpha$-abstraction of methane to generate the transient imido complex $Cp_2Zr{=}NR$ followed by rapid reaction with the amine to provide the bis(amide) (Scheme I). Thus methyl amide **2a** arises from protonation of the zirconium-bound methyl group by the amine, but loss of the second equivalent of methane from **2a** proceeds via an $\alpha$-abstraction pathway, as indicated by the kinetic experiments discussed above. This change in mechanism is probably a result of substitution of an amide group for a methyl group in $Cp_2ZrMe_2$. The larger amide ligand increases the steric hindrance about the zirconium center favoring $\alpha$-abstraction to form the less sterically crowded imido intermediate while decreasing its Lewis acidity through $\pi$-donation of the nitrogen lone pair to the zirconium center.[24]

**Trapping of $Cp_2Zr{=}NR$ with Lewis Bases.** Thermolysis of the alkyl amides $Cp_2Zr(NHR)(R')$ (**2a–d**) or the bis(amides) $Cp_2Zr(NHR)_2$ (**3b–c**) induces an $\alpha$-abstraction of alkane R′H or amine $RNH_2$, respectively, to generate the transient imido complexes **1a–d**. The fate of **1a–d** is largely governed by the size and electronic properties of the *N*-alkyl/aryl group. For example heating the alkyl amide **2a** in $C_6H_6$ or THF resulted in formation of the bridging imido dimer **4a** (Scheme II, Figure 1). Formation of **4a** presumably arises via dimerization of two molecules of **1a**. In contrast, heating alkyl amides **2b–d** to 85 °C in THF leads to the more highly hindered imido complexes **1b–d** which were trapped by the solvent to provide the coordinatively saturated monomeric imido complexes $Cp_2Zr(NR)(THF)$ (**5b–d**) in 71, 69, and 76% isolated yields (eq 3). Similar methodology was utilized by Cummins, Baxter, and Wolczanski to trap the bis(amide) imido complex $((Me_3C)_3SiNH)_2Zr{=}NSi(CMe_3)_3$

---

[24] Hillhouse, G. L.; Bulls, A. R.; Santarsiero, B. D.; Bercaw, J. E. *Organometallics* 1988, 7, 1309.

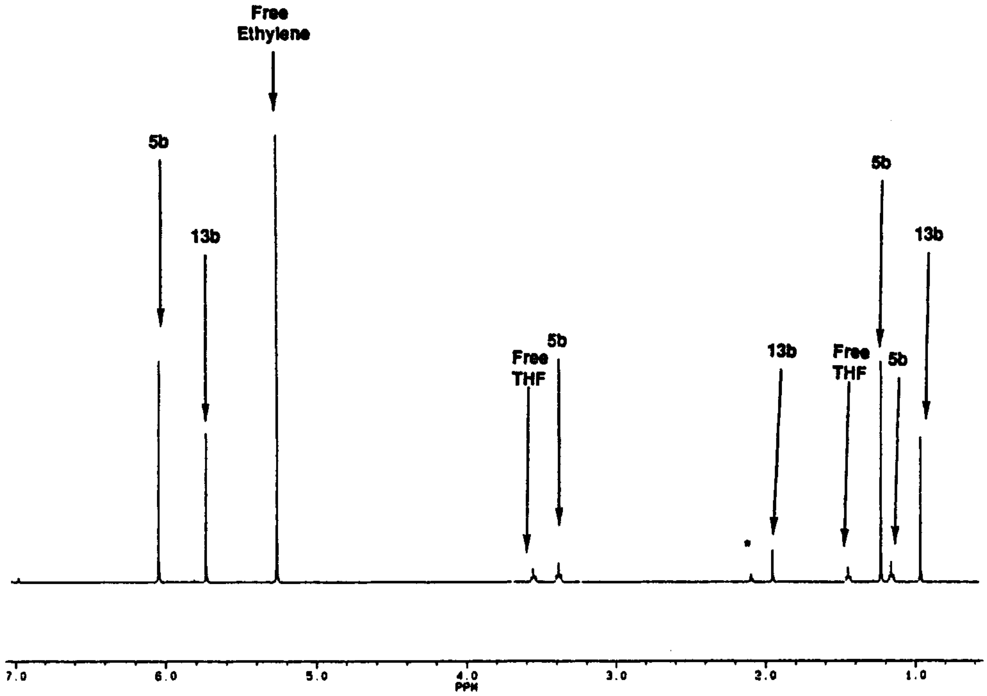

**Figure 5.** $^1$H NMR spectrum of the equilibrium mixture of free ethylene, **5b**, free THF, and **13b** at 10 °C in toluene-$d_8$. Residual $C_6H_5$–$CD_2H$ is marked with an asterisk.

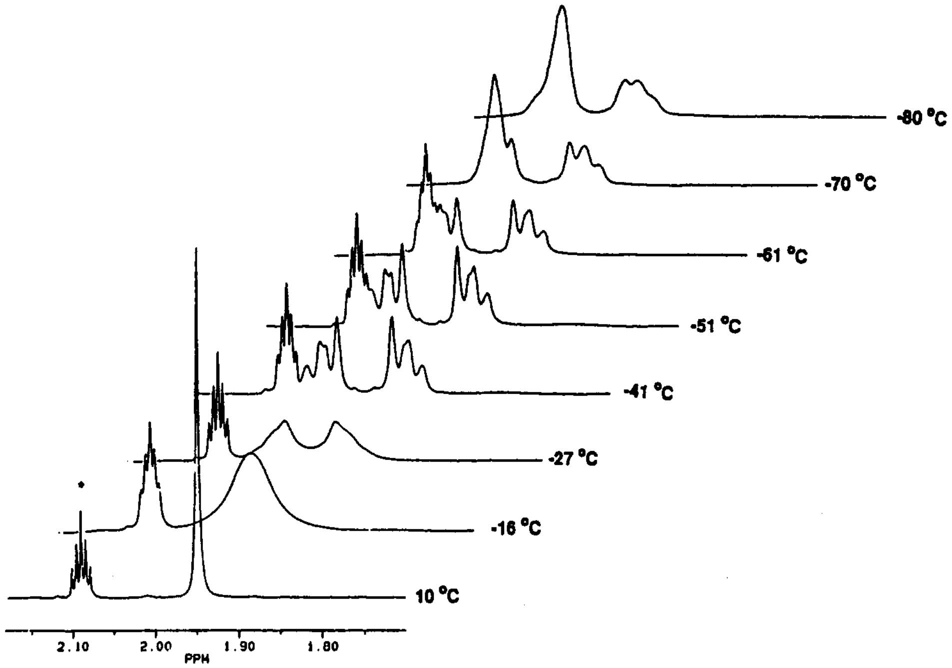

**Figure 6.** Variable temperature $^1$H NMR spectra (400 MHz) of **13b** in toluene-$d_8$ illustrating the methylene region. The starred peak is $C_6D_5$–$CD_2H$.

as its THF adduct.[2] The zirconium imido complexes synthesized in our laboratories and Wolczanski's represent the first group IV monomeric imido complexes to be isolated. Since our preliminary reports of these observations[1,2] a number of new imido complexes of this group have been reported.[3]

A correlation of the electronic structure of *tert*-butyl imido ligands with the difference in the $^{13}$C NMR chemical shifts of the $\alpha$ and $\beta$ carbons of the N-*tert*-butyl group (defined as the quantity $\Delta\delta$) has been proposed by Nugent et al.[25] The value of $\Delta\delta$ is believed to reflect the $\pi$ bond order of the M–NCMe$_3$ linkage; a decrease in $\Delta\delta$ reflects a decrease in $\pi$ bond order. The value of $\Delta\delta$ for the imido complexes **5b** and **6b** are 28 and 27 ppm, respectively. These values of $\Delta\delta$ for **5b** and **6b** are among the lowest known, suggesting that the group IV imido complexes have the lowest $\pi$-bond order. The linearity of the M–N–R linkage observed in nearly all crystallographically characterized compounds containing this ligand has been attributed[4] to the ability of the imido functionality to act as a 4 electron donor (2 single electrons and a lone pair). On the basis of this formalism, the electron count of complexes **5b** (Figure 2) and **6b** could be considered to be 20 electrons. The strength of early transition metal oxygen and nitrogen bonds (such as alkoxides and amides) has traditionally been attributed, in part, to donation of

---

(25) Nugent, W. A.; McKinney, R. J.; Kasowski, R. V. Van-Catledge, F. A. *Inorg. Chim. Acta* **1982**, *65*, L91.

Scheme VI

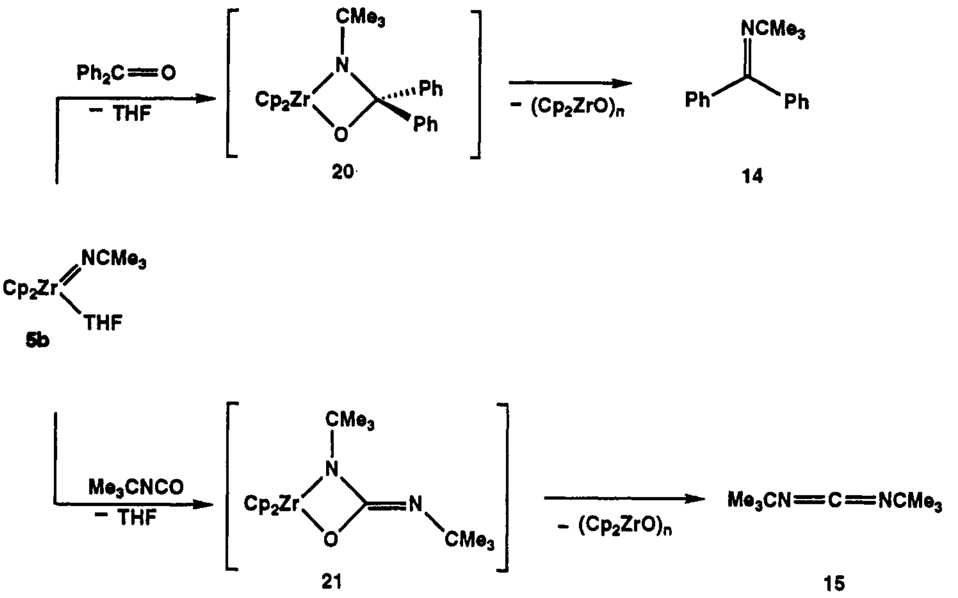

Scheme VII

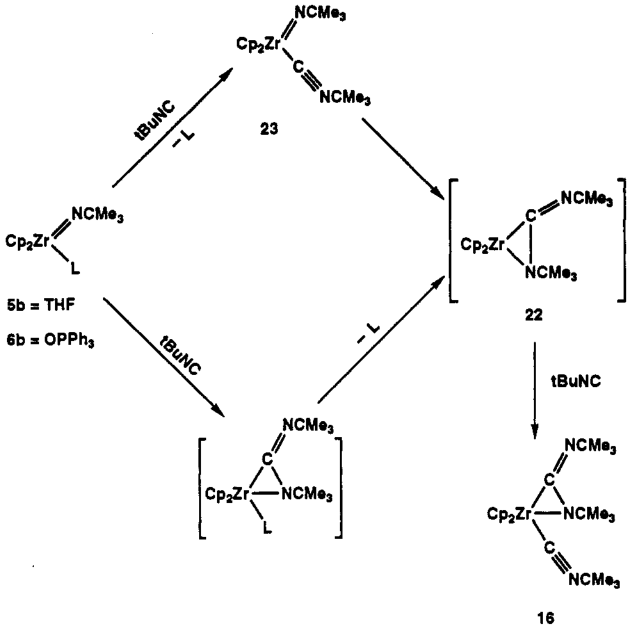

Scheme VIII

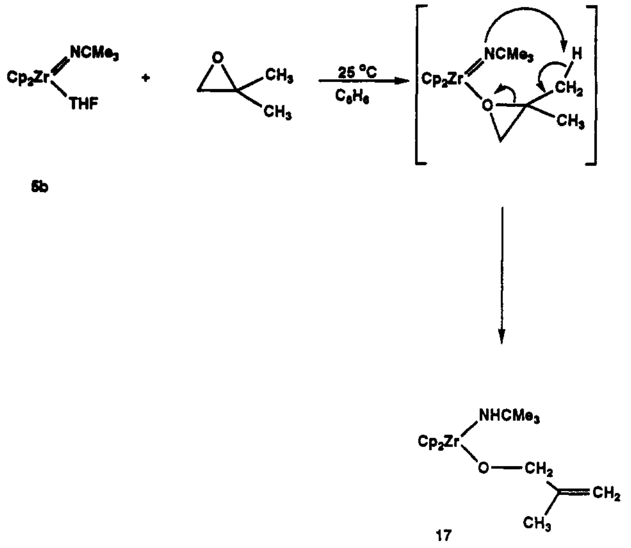

Scheme IX

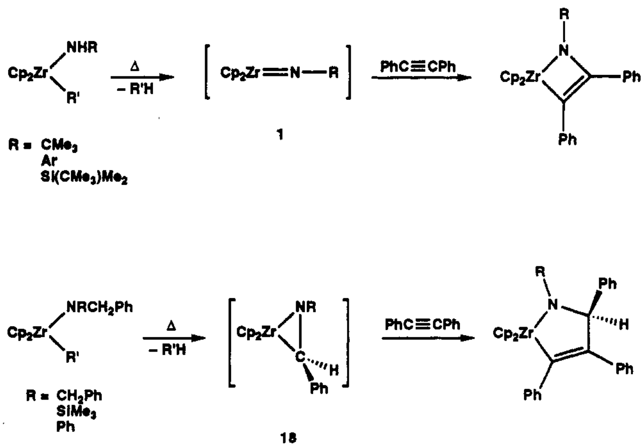

the lone pair of these ligands to empty orbitals on the metal center.[26] Recently, Bercaw and co-workers have postulated[24] that there is interaction of the amide lone pair of $Cp^*_2Hf(NHMe)(H)$ with the metal on the basis of the orientation of the Hf–N(Me)H moiety in the crystal. However, they found no evidence for this interaction in solution by variable temperature NMR spectrometry, suggesting that the barrier to rotation about the Hf–N bond (and thus the strength of the donation of the lone pair to the hafnium) is under 10 kcal/mol.

It has been suggested that although the imido ligands are linear, the electron density remains largely on the nitrogen rather than in the M–N $\pi$-bonds.[27] In contrast, calculations on the closely related complex $Cp^*_2VNAr$ by Osborne and Trogler suggest the presence of a V–N triple bond.[28,29] Clearly, more work is needed to resolve these differing pictures of metal–imido bonding.

**Addition of C—H and N—H Bonds across the Zr=N Linkage.** When the alkyl amides **2b** and **2d** were heated

---

(26) Cardin, D. J.; Lappert, M. F.; Raston, C. L.; Riley, P. I. In *Comprehensive Organometallic Chemistry*; Wilkinson, G., Ed.; Pergamon Press: Oxford, U.K., 1982; Vol. 3, p 587.

(27) (a) Anhaus, J. T.; Kee, T. P.; Schfield, M. H., Schrock, R. R. *J. Am. Chem. Soc.* **1990**, *112*, 1642. (b) Jørgenson, K. A. *Inorg. Chem.* **1993**, *32*, 1521.

(28) Osborne, J. H.; Trogler, W. C. *J. Am. Chem. Soc.* **1985**, *107*, 7945.

(29) Reference 4, p 42.

**Scheme X**

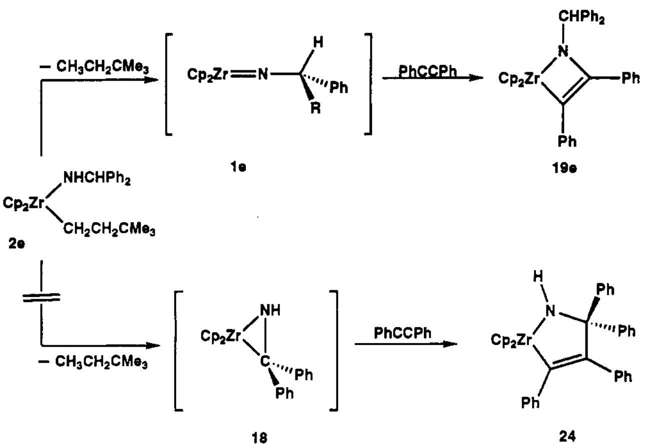

to 85 °C in benzene in the absence of trapping ligands, the phenyl amides $Cp_2Zr(NHCMe_3)(Ph)$ (**7b**) and $Cp_2Zr(NHSi(CMe_3)Me_2)(Ph)$ (**7d**) were isolated (eq 5). Similarly, heating the monomeric imido complex **5b** in benzene also resulted in formation of the phenyl amide **7b** (eq 6). Apparently, the Zr=N linkage in **1b** and **1d** are sufficiently reactive to cleave the $sp^2$ hybridized C—H bond of benzene. However, attempts to activate the $sp^3$ C—H bond of methane by heating a cyclohexane solution of **5b** under 18 atm of methane led to intractable products. Thermolysis of the silylamide **2d** with methane also led to intractable products. In comparison, Cummins, Baxter, and Wolczanski have found that the imido complex $(t\text{-}Bu_3SiNH)_2Zr{=}NSi(t\text{-}Bu)_3$ generated from the tris(amide) alkyl zirconium complexes $(t\text{-}Bu_3SiNH)_3ZrR$ (R = Me, cyclohexyl) possesses the ability to activate even the $sp^3$ hybridized C—H bonds of methane.[2] The increased reactivity of the bis(amide) imido complex $(t\text{-}Bu_3SiNH)_2Zr{=}NSi(t\text{-}Bu)_3$ toward C—H bonds is probably related to the greater unsaturation of the metal center.

Another factor besides the degree of saturation of the metal center which affects the reactivity of the Zr—NR functionality toward C—H bonds is the nature of the R group. For example, heating a benzene solution of the alkyl arylamide **2a** led only to imido dimer **4a**. Similarly, thermolysis of the more hindered arylamide **2c** led to formation of neohexane ($^1H$ NMR spectrometry) but did not result in formation of the C—H activation product $Cp_2Zr(NH(2,6\text{-}Me_2C_6H_3))(Ph)$ (**7c**), giving intractable products instead. However, heating **2b** or **2d**, which have alkyl and silyl rather than aryl groups attached to nitrogen, provided the C—H activation products **7b** and **7d**.

It is possible that **7c** was formed from **2c** but was unstable to the reaction conditions and decomposed. To examine this possibility, **7c** was independently synthesized. Heating $Cp_2ZrPh_2$ in benzene at 85 °C (which were the same conditions used in the attempted C–H activation with **2c**) with 2,6-dimethylaniline resulted in the formation of **7c**. The stability of **7c** to the conditions of this reaction indicates that this complex was not formed in the thermolysis of **2c**.

We believe the inability of the arylimido complex $Cp_2Zr{=}N$(2,6-dimethylphenyl) to activate the C—H bonds of benzene, as observed for the alkyl- and silylimido complexes $Cp_2Zr{=}NCMe_3$ and $Cp_2Zr{=}NSi(CMe_3)Me_2$, suggests that the aryl group deactivates the Zr—N linkage by accepting electron density through resonance delocalization.

Although the C—H activation processes discussed above represent a new class of reactions the addition of more polar HX bonds across the metal imido functionality has been documented for a number of X groups.[30] The stability of the imido ligand toward addition of HX bonds varies dramatically. For example, the imido complex $(MeCN)_2Ta(NR)(Cl_3)$ has been reported to be stable to HCl in ether.[31] In contrast, we have found that even the weakly acidic N—H bonds of amines will add across the zirconium imido functionality. Thus, addition of 2,6-dimethylaniline to the imido complex **5c** resulted in the rapid formation of the bis(amide) **3c** in >98% yield by $^1H$ NMR integration against an internal standard (eq 7). It is interesting to compare the zirconium imido–bis(amide) complex interconversion with different systems. For example, the equilibrium between the bis(amide) complex $Cp_2Zr(NHR)_2$ and the imido complex $Cp_2Zr{=}NR$ and $RNH_2$ lies very far to the left. In contrast, Rothwell and co-workers observed (Figure 3) that upon addition of 4-pyrrolidinopyridine (py′) to either $Zr(NH(2,6\text{-}i\text{-}Pr_2C_6H_3))_4$ or $Zr(NHPh)_2(O(2,6\text{-}i\text{-}Pr_2C_6H_3))_2$ these complexes eliminate amine to provide $(py')_2Zr(NH(2,6\text{-}i\text{-}Pr_2C_6H_3))_2({=}N(2,6\text{-}i\text{-}Pr_2C_6H_3))$ or $(py')_2Zr({=}NPh)(O(2,6\text{-}i\text{-}Pr_2C_6H_3))_2$.[3] In the late transition metal imido complexes ($\eta^6$-arene)OsNR and Cp*IrNR, addition of amine $R'NH_2$ results in exchange of the NR moiety to give ($\eta^6$-arene)OsNR′ and Cp*IrNR′ and $RNH_2$; these reactions probably proceed through bis(amide) intermediates.[32]

**Reactions of $Cp_2Zr{=}NR$ with Alkynes and Olefins.** When the alkyl amide (**2a–d**) or the bis(amide) complexes (**3b** and **3c**) are heated (85–120 °C) with internal alkynes, azametallacyclobutenes are formed (Scheme IV). In the case of the bis(amides), thermolysis in the presence of an excess of alkyne and the corresponding amine resulted in the catalytic hydroamination of alkynes.[10]

The isolated (but labile) THF-substituted imido complexes **5b–d** can be used to regenerate their reactive nonligated analogues **1b–d** at 25 °C rather than at the higher temperatures required for thermolysis of the alkyl amide or bis(amide) complexes (85–120 °C). An example of the importance of this is the reaction of the alkyl amide **2c** with 4,4-dimethyl-2-pentyne. At the temperature required to induce $\alpha$-abstraction of methane from **2c** (85 °C) the metallacycle which is formed via cycloaddition of 4,4-dimethyl-2-pentyne was unstable and led to a multitude of products. In contrast, addition of 4,4-dimethyl-2-pentyne to the imido complex **5c** resulted in the rapid formation of the purple metallacycle **9c** (eq 8).

Another example of the utility of the imido complex **5b** was illustrated in reactions with terminal alkynes. Zirconium amides have been shown to react with terminal alkynes to provide $\sigma$-acetylides in high yield.[33] On the basis of this precedent, phenylacetylene might be expected to react with methyl amide **2b** to provide the methyl acetylide $Cp_2Zr(Me)(CCPh)$ and free amine, precluding synthesis of monosubstituted azametallacycles in this manner. However, addition of phenylacetylene to the monomeric imido complex **5b** resulted in formation of the purple metallacycle **10b** with the regiochemistry illustrated in eq 8.

Under the conditions employed in the synthesis of azametallacyclobutenes from the imido complexes **5b–c**

---

[30] Reference 4, pp 223–229.

[31] Cotton, F. A.; Hall, W. T. *J. Am. Chem. Soc.* **1979**, *101*, 5094.

[32] (a) Michelman, R. I.; Andersen, R. A.; Bergman, R. G. *J. Am. Chem. Soc.* **1991**, *113*, 5100. (b) Michelman, R. I.; Bergman, R. G.; Andersen, R. A., submitted for publication.

[33] Chandra, G.; Lappert, M. F.; Srivastava, R. C. *J. Chem. Soc. A* **1968**, 1940.

(<5 min, 25 °C) formation of the metallacycles is not reversible. However, when the metallacycle **8c** is heated to 45 °C with di-*p*-tolylacetylene, an equilibrium between the metallacycles **8c** and **11c** and the diarylacetylenes was established over several days, as shown in eq 9. This most likely occurs via retrocyclization of the metallacycle to generate the intermediate **1c** which can react with either of the diarylacetylenes. In a similar manner the THF-substituted imido complex **5b** reacts reversibly with olefins. Due to the greater strength of the $\pi$-bond of an olefin relative to the strength of the last $\pi$-bond of an alkyne[34] and the greater strength of an $sp^2$ compared to an $sp^3$ Zr–C bond,[35] the azametallacyclobutanes are more labile than the azametallacyclobutenes. Thus, addition of 3 equiv of norbornene to **5b** led to an equilibrium mixture of **5b**, norbornene, azametallacyclobutane **12b**, and THF (eq 10). Because $K_{eq}$ favors the starting materials, addition of a large excess of norbornene is required to drive the equilibrium to azametallacyclobutane at room temperature.

In the 10 °C $^1H$ NMR spectrum (Figure 5) of **13b**, derived from addition of ethylene to **5b** (Scheme V), a single resonance was observed for the methylene groups of **13b**. Because the resonances for free and bound ethylene are separated by over 3 ppm in the $^1H$ NMR spectrum, it is clear that there is no exchange between them on the NMR time scale. However, when the mixture was cooled, the singlet assigned to the $CH_2$ groups ($\delta$ 1.94 ppm) broadened and decoalesced into two multiplets (Figure 6). In the $^{13}C\{^1H\}$ NMR spectrum at −40 °C the methylenes were inequivalent and the cyclopentadienyl ligands equivalent, suggesting that the static structure is that of metallacycle **13b** (Scheme V). We believe that the exchange process involves rapid and reversible formation of the imido ethylene complex $Cp_2Zr({=}NR)(CH_2{=}CH_2)$ as a transient intermediate.[36] This transient olefin complex then undergoes rotation of the bound ethylene, interconverting the methylenes. Olefin complexes of *formally* $d^0$ metal centers have been considered in a number of transformations, but there are no examples of such complexes which have been characterized.[37] However, complexes containing zirconium *formally* in the +4 oxidation state have been observed to act as $\pi$-donors as well as Lewis acids. For example, a decrease in $\nu_{CO}$ (from free CO at $\nu$ = 2143 to 2044 cm$^{-1}$) was observed by Bercaw and co-workers in the coordination of CO to $Cp^*{}_2ZrH_2$ at low temperature and was explained by $\pi$-donation from the formally $Zr^{IV}$ metal center.[38]

**Reactions of $Cp_2Zr(NCMe_3)(THF)$ with C=O Bonds.** The $\Delta\delta$ values derived from the $^{13}C$ NMR spectrometry (discussed above) have been used to predict the reactivity of the metal *tert*-butylimido functionality toward organic carbonyls. For example, metal imido complexes with a $\Delta\delta < 50$ have been observed to react with benzaldehyde via metathesis to provide the imine of benzaldehyde and the corresponding metal oxo complex. Because the imido complexes **5b** and **6b** have $\Delta\delta$ values of 28 and 27, they are expected to react rapidly with aldehydes. However, the reactive intermediate in this process is most likely the ligand free imido complex **1b** in which case the $\Delta\delta$ values of **5b** and **6b** do not apply. We found that treatment of **5b** with a slight excess of benzophenone or *tert*-butyl isocyanate resulted in the rapid formation of the *tert*-butylimine of benzophenone (**14**) in 89% and 1,3-di-*tert*-butylcarbodiimide (**15**) in 65% yield (Scheme VI). This transformation is reminiscent of Wittig reactions between phosphonium ylides and aldehydes and ketones, and most likely follows a similar pathway. We assume that it is initiated by loss of the coordinated THF ligand of **5b** and coordination of the organic carbonyl. This is followed by intramolecular attack of the imido functionality on the $\eta^1$-carbonyl group which leads to formation of intermediates **20** and **21** (Scheme VI). The intermediates **20** and **21** then undergo retrocyclization to provide the organic products and zirconium oxides. Similar mechanisms have been proposed for the reaction of early transition metal alkylidenes with organic carbonyls[39] which were also reported to display enhanced reactivity relative to phosphonium ylides.[40,41] Similarly, the imido complex **5b** demonstrated greater reactivity than phosphine imines toward benzophenone: $n\text{-}Bu_3P{=}NCMe_3$[42] failed to react with benzophenone after 7 days at 85 °C.

**Reaction of the Monomeric Imido Complexes with *tert*-Butyl Isocyanide and Isobutylene Oxide.** The monomeric imido complexes also undergo coupling/trapping reactions with isocyanides. Addition of 2 equiv of *tert*-butyl isocyanide to **5b** resulted in the rapid formation of the $\eta^2$-carbodiimide isocyanide complex **16** (Scheme VII). The mechanism of this transformation most likely involves initial formation of the intermediate $\eta^2$-carbodiimide complex (**22**) $Cp_2Zr(N(CMe_3)C{=}NCMe_3)$ which is trapped by additional isocyanide. The formation of **22** could be envisioned to occur by either direct attack of the isonitrile on the imido ligand in a fashion analogous to the addition of a carbene to an olefin. Alternatively, initial loss of the THF ligand and coordination of the isocyanide to generate **23** followed by formation of a C—N bond to give **22** is also possible (Scheme VII). When the imido complex **5b** was allowed to interact with only 1 equiv of isocyanide, the $\eta^2$-carbodiimide isocyanide complex **16** was formed in 50% yield, with half of the imido complex **5b** remaining unreacted. This observation indicates that trapping of **22** with isocyanide occurs more rapidly than

---

(34) The bond energies of C–C single, double, and triple bonds are 81, 148, and 194 kcal/mol, respectively; see: Lowry, T. H.; Schueller Richardson, K. *Mechanism and Theory in Organic Chemistry*; Harper & Row, Publishers: New York, 1987; p 162.

(35) The bond energy of the $sp^2$ Zr–C bond of $Cp^*{}_2ZrPh_2$ was determined to be 6 kcal/mol greater then the $sp^3$ Zr–C bond of $Cp^*{}_2ZrMe_2$; see: Schock, L. E.; Marks, T. J. *J. Am. Chem. Soc.* **1988**, *110*, 7701.

(36) For a theoretical analysis of a related process involving $Cp_2Ti({=}CH_2)(CH_2{=}CH_2)$ see: (a) Upton, T. H.; Rappé, A. K. *J. Am. Chem. Soc.* **1985**, *107*, 1206. (b) Eisenstein, O.; Hoffmann, R.; Rossi, A. R. *J. Am. Chem. Soc.* **1981**, *103*, 5582. (c) McKinney, R. J.; Tulip, T. H.; Thorn, D. L.; Tebbe, F. N. *J. Am. Chem. Soc.* **1981**, *103*, 5584. Similar results were found for group VI metallacyclobutanes; see: (d) Rappé, A. K.; Goddard, W. A. *J. Am. Chem. Soc.* **1982**, *104*, 448. (e) Note added in proof: Imidovanadium complexes have recently been shown to react reversibly with ethylene: de With, J.; Horton, A. D.; Orpen, A. G. *Organometallics* **1993**, *12*, 1493.

(37) (a) Nelson, J. E.; Bercaw, J. E.; Labinger, J. A. *Organometallics* **1989**, *8*, 2484. (b) Jeske, G.; Luake, H.; Maueramann, H.; Swepston, P. N.; Schumann, H.; Marks, T. J. *J. Am. Chem. Soc.* **1985**, *107*, 8091. (c) Thompson, M. E.; Baxter, S. M.; Bulls, A. R.; Burger, B. J.; Nolan, M. C.; Santarsiero, B. D.; Schaefer, W. P.; Bercaw, J. E. *J. Am. Chem. Soc.* **1987**, *109*, 203. (d) McAlister, D. R.; Erwin, D. K.; Bercaw, J. E. *J. Am. Chem. Soc.* **1978**, *100*, 5966.

(38) (a) Manriquez, J. M.; McAlister, D. R.; Sanner, R. D.; Bercaw, J. E. *J. Am. Chem. Soc.* **1976**, *98*, 6733. (b) Manriquez, J. M.; McAlister, D. R.; Bercaw, J. E. *J. Am. Chem. Soc.* **1978**, *100*, 2716.

(39) (a) Schrock, R. R. *J. Am. Chem. Soc.* **1976**, *98*, 5399. (b) Aguero, A.; Kress, J.; Osborn, J. A. *J. Chem. Soc., Chem. Commun.* **1986**, 531. (c) Kauffmann, T.; Ennen, B.; Sander, J.; Wieschollek, R. *Angew. Chem., Int. Ed. Engl.* **1983**, *22*, 244.

(40) Wittig, G. *J. Organomet. Chem.* **1975**, *100*, 279.

(41) (a) Tebbe, F. N.; Parshall, G. W.; Reddy, G. S. *J. Am. Chem. Soc.* **1978**, *100*, 3611. (b) Pine, S. H.; Zahler, R.; Evans, D. A.; Grubbs, R. H. *J. Am. Chem. Soc.* **1980**, *102*, 3270. (c) Brown-Wenseley, K. A.; Buchwald, S. L.; Cannizzo, L.; Clawson, L.; Ho, S.; Meinhardt, D.; Stille, J. R.; Straus, D.; Grubbs, R. H. *Pure Appl. Chem.* **1983**, *55*, 1733.

(42) Zimmerman, H.; Singh, G. *J. Org. Chem.* **1963**, *28*, 483.

reaction of the monomeric imido complex with isocyanide. Surprisingly, in contrast to the reaction of triphenylphosphine oxide adduct **6b** with alkynes, which was slow relative to the reaction of THF adduct **5b**, reaction of **6b** with *tert*-butyl isocyanide led to production of **16** in seconds. An analogous coupling/trapping reaction was observed with the iridium imido complex $Cp^*IrN(CMe_3)$ which gives $Cp^*Ir(N(CMe_3)C{=}NCMe_3)(CNCMe_3)$.[43]

Epoxides have been found to react with the imido complex **5b** to give ring-opened products containing strong Zr–O $\sigma$-bonds. As shown in Scheme VIII, the reaction of **5b** with isobutylene oxide led to the allylic alkoxide amide complex $Cp_2Zr(NHCMe_3)(OCH_2C(CH_2)CH_3)$ (**17**). The mechanism of this transformation most likely involves initial substitution of THF by the epoxide at the zirconium center (Scheme VIII). The Lewis acidity of the Zr center should increase the Bronsted acidity of the methyl groups on the coordinated isobutylene oxide. One of these methyl protons can then be removed by the imido ligand, opening the epoxide to provide **17**. Analogous conversions of epoxides to allylic alcohols[44] have been promoted both by strong bases such as lithium diethylamide[45] and Lewis acids like dialkylboryl triflate[46] or diethylaluminum dialkylamide.[47]

**$\alpha$- vs $\beta$-Abstraction; Preference for Generation of Zirconium Imido or $\eta^2$-Imine Complexes.** As noted in the Results, zirconium alkyl amides have been observed to undergo both $\alpha$- and $\beta$-extrusion of alkane (Scheme IX) but in no case have the alkyl amides examined contained both $\alpha$- and $\beta$-hydrogens. This led us to prepare the alkyl amide $Cp_2Zr(NHCHPh_2)(CH_2CH_2CMe_3)$ (**2e**). Thermolysis of **2e** with 4 equiv of diphenylacetylene for 24 h at 115 °C resulted in the formation the azametallacyclobutene **19e** (Scheme X), indicating that $\alpha$-abstraction to form the imido intermediate **1e** predominates over $\beta$-abstraction which would lead to azametallacyclopropane **18** followed by trapping with diphenylacetylene, giving the azametallacyclopentene **24**.

## Experimental Section

**General Information.** Unless otherwise noted, all manipulations were carried out under an inert atmosphere in a Vacuum Atmospheres 553-2 drybox with attached M6-40-1H Dritrain or by using standard Schlenk or vacuum line techniques. Solutions were degassed as follows: they were cooled to −196 °C, evacuated under high vacuum, and thawed. This sequence was repeated three times in each case. Glass reaction vessels fitted with ground glass joints and Teflon stopcocks are referred to as "bombs" throughout the Experimental Section.

$^1H$ NMR spectra were obtained on either the 250-, 300-, 400-, or 500-MHz Fourier transform spectrometers at the University of California, Berkeley (UCB) NMR facility. The 250- and 300-MHz instruments were constructed by Mr. Rudi Nunlist and interfaced with either a Nicolet 1180 or 1280 computer. The 400- and 500-MHz instruments were commercial Bruker AM series spectrometers. $^1H$ NMR spectra were recorded relative to residual protiated solvent. $^{13}C$ NMR spectra were obtained at either 75.4 or 100.6 MHz on the 300- or 400-MHz instruments, respectively, and chemical shifts were recorded relative to the solvent resonance. Chemical shifts are reported in units of parts per million downfield from tetramethylsilane and all coupling constants are reported in hertz.

IR spectra were obtained on a Nicolet 510 FT-IR spectrometer. Mass spectroscopic (MS) analyses were obtained at the UCB mass spectrometry facility on AEI MS-12 and Kratos MS-50 mass spectrometers. Elemental analyses were obtained from the UCB Microanalytical Laboratory.

Sealed NMR tubes were prepared using Wilmad 505-PP and 504-PP tubes attached via Cajon adapters directly to Kontes vacuum stopcocks and degassed using three freeze–pump–thaw cycles before flame sealing.[48] Known volume bulb vacuum transfers were accomplished with an MKS Baratron attached to a high vacuum line.

Unless otherwise specified, all reagents were purchased from commercial suppliers and used without further purification. 2,6-Dimethylaniline, 4-*tert*-butylaniline, and (diphenylamino)methane (Aldrich) were dried over sodium and distilled under vacuum. *tert*-Butylamine was refluxed over $CaH_2$ and vacuum transferred. Norbornene was vacuum transferred from sodium. Phenylacetylene and *tert*-butyl isocyanide (Aldrich) were distilled from $P_2O_5$. Isobutylene oxide was distilled from $CaH_2$ under reduced pressure. Diphenyl- and di-*p*-tolylacetylene (Aldrich) were used without purification. All lithium amides, LiNHR, were prepared by deprotonating the parent amine with 1.0 equiv of *n*-BuLi. In some cases the lithium amides were isolated by removing the volatile materials and were used as solids, and in others the lithium amides were generated and used in solution (see below for specific examples).

Pentane and hexanes (UV grade, alkene free) were distilled from sodium benzophenone ketyl/tetraglyme under nitrogen. Benzene, toluene, ether, and THF were distilled from sodium benzophenone ketyl under nitrogen. Deuterated solvents for use in NMR experiments were dried in the same manner as their protiated analogues but were vacuum transferred from the drying agent. $Cp_2ZrMe_2$,[11] $Cp_2Zr(Me)(Cl)$,[1,7] $Cp_2Zr(CH_2CH_2CMe_3)(Cl)$,[8] $H_2NSi(CMe_3)Me_2$,[49] $Cp_2ZrPh_2$,[50] and $Cp_2Zr(\eta^2\text{-}C_6H_4)(PMe_2Ph)$[17] were prepared by literature methods. The synthesis of compounds **8b**, **8c**, **9c**, and **11c** are described elsewhere.[10]

**$Cp_2Zr(NH(4\text{-}CMe_3C_6H_4))(Me)$ (2a).** To a stirred solution of $Cp_2Zr(Me)(Cl)$ (248 mg, $9.12 \times 10^{-4}$ mol) in 25 mL of THF was added 1.1 equiv of $LiNH\text{-}4\text{-}CMe_3C_6H_4$ as a solution in 5 mL of THF. The addition was performed in a dropwise fashion over 5 min at 25 °C. The solution was stirred for 12 h at 25 °C, during which time it became bright yellow and the solvent was removed under vacuum to yield a yellow solid. The solid product was extracted into 6 mL of toluene, and the solution was filtered to remove the LiCl. The toluene was removed under reduced pressure, the remaining solid was dissolved in 4 mL of hexanes, and the resulting solution was cooled to −30 °C. Small light yellow crystals grown in this fashion were collected by decanting off the solvent and washing with cold hexanes to yield 245 mg ($6.36 \times 10^{-4}$ mol, 70%). IR ($C_6H_6$): 3342 (w), 2962, 2926, 2871, 1604, 1508, 1445, 1297, 1263, 1224, 1186, 862, 834, 805 cm$^{-1}$. Anal. Calcd for $C_{21}H_{27}NZr$: C, 65.57; H, 7.07; N, 3.64. Found: C, 65.47; H, 6.98; N, 3.58.

**$Cp_2Zr(NHCMe_3)(Me)$ (2b).** Under a nitrogen atmosphere $LiNHCMe_3$ (65.6 mg, $8.30 \times 10^{-4}$ mol) was dissolved in 5 mL of THF. This solution was added in a dropwise fashion to 25 mL of THF containing $Cp_2Zr(Me)(Cl)$ (197 mg, $7.25 \times 10^{-4}$ mol) at 25 °C over a 5-min period. The reaction was then stirred for 2.5 h at room temperature followed by removal of the solvent under reduced pressure. The remaining solid was extracted into hexanes, the mixture was filtered to remove the LiCl, and the hexanes were removed under vacuum to give **2b** as a white solid

---

[43] Glueck, D. S.; Hollander, F. J.; Bergman, R. G. *J. Am. Chem. Soc.* **1989**, *111*, 2719.

[44] For a review see: Crandall, J. K.; Apparu, M. *Org. React.* **1983**, *29*, 345.

[45] (a) Cope, A. C.; Brown, M.; Lee, H. H. *J. Am. Chem. Soc.* **1958**, *80*, 2855. (b) Crandall, J. K.; Chang, L. H. *J. Org. Chem.* **1967**, *32*, 435. (c) Thummel, R. P.; Rickborn, B. *J. Org. Chem.* **1971**, *36*, 1365. (d) Kissel, C. L.; Rickborn, B. *J. Org. Chem.* **1972**, *37*, 2060.

[46] Inoue, T.; Uchimaru, T.; Mukaiyama, T. *Chem. Lett.* **1977**, 1215.

[47] Yamamoto, H.; Nozaki, H. *Angew. Chem., Int. Ed. Engl.* **1978**, *17*, 169.

[48] Bergman, R. G.; Buchanan, J. M.; McGhee, W. D.; Periana, R. A.; Seidler, P. F.; Trost, M. K.; Wenzel, T. T. In *Experimental Organometallic Chemistry: A Practicum in Synthesis and Characterization*; Wayda, A. L., Darensbourg, M. Y., Eds.; ACS Symposium Series 357; American Chemical Society: Washington, DC, 1987; p 227.

[49] Bowser, J.; Neilson, R. H.; Wells, R. L. *Inorg. Chem.* **1978**, *17*, 1882.

[50] Samuel, E.; Rousch, M. D. *J. Am. Chem. Soc.* **1973**, *95*, 6263.

in 80–95% yield that was used without further purification. IR ($C_6H_6$): 3310 (w), 2960, 2925, 1445, 1371, 1356, 1206, 980, 799 cm$^{-1}$. Anal. Calcd for $C_{15}H_{23}NZr$: C, 58.39; H, 7.51; N, 4.54. Found: C, 58.07; H, 7.47; N, 4.32.

**$Cp_2Zr(CH_2CH_2CMe_3)(NH(2,6\text{-}Me_2C_6H_3))$ (2c).** To a flask containing $Cp_2Zr(CH_2CH_2CMe_3)(Cl)$ (1.60 g, 4.68 × $10^{-3}$ mol) and 70 mL of THF was added solid $LiNH(2,6\text{-}Me_2C_6H_3)$ (1.34 g, 1.05 × $10^{-2}$ mol, 2.25 equiv) at room temperature. The resulting mixture was stirred for 15 h and the solvent removed under reduced pressure. The remaining yellow solid was extracted into 30 mL of ether, and the resulting mixture was filtered to remove LiCl and excess lithium amide. Concentrating the filtrate to 15 mL under reduced pressure followed by cooling to −30 °C provided yellow crystals of **2c** which were isolated by filtration and washed with cold ether to yield 1.43 g (3.37 × $10^{-3}$ mol, 72%). IR ($C_6H_6$): 3303 (w), 2948, 2898, 2860, 2361, 1652, 1559, 1540, 1521, 1507, 1488, 1464, 1444, 1437, 1423, 1420, 1386, 1358, 1254, 1229, 1216, 1093, 1016, 859, 803 (s), 764, 737, 702, 562, 506 cm$^{-1}$. Anal. Calcd for $C_{24}H_{31}NZr$: C, 67.55; H, 7.79; N, 3.28. Found: C, 67.15; H, 7.83; N, 3.39.

**$Cp_2Zr(NHSi(CMe_3)Me_2)(CH_2CH_2CMe_3)$ (2d).** To a solution of $H_2NSi(CMe_3)Me_2$ (218 mg, 1.66 × $10^{-3}$ mol) in 10 mL of THF was added 0.72 mL of 2.3 M *n*-BuLi in hexanes (1.66 × $10^{-3}$ mol) at 25 °C. The resulting solution of $LiNHSi(CMe_3)Me_2$ was treated with $Cp_2Zr(CH_2CH_2CMe_3)(Cl)$ (473 mg, 1.38 × $10^{-3}$ mol). The solution was stirred for 10 h, and the solvent was removed under reduced pressure. The remaining solid was extracted into 12 mL of hexanes, and the resulting solution filtered and concentrated to 4 mL under vacuum. Hexamethyldisiloxane (4 mL) was added, and the solution was cooled to −30 °C. Crystals of **2d** were isolated by decanting off the solvent and washing the clear crystals with 5 mL of hexamethyldisiloxane to yield 434 mg (9.94 × $10^{-4}$ mol, 72%). IR (Nujol): 3332 (w), 1358, 1243, 1235, 1044, 1015, 989 (s), 887, 873, 820, 797 (s), 783, 746, 722, 666, 650, 574 cm$^{-1}$. Anal. Calcd for $C_{22}H_{39}NSiZr$: C, 60.49; H, 9.00; N, 3.21. Found: C, 60.61; H, 8.96; N, 3.05.

**$Cp_2Zr(CH_2CH_2CMe_3)(NHCHPh_2)$ (2e).** To a solution of $H_2NCHPh_2$ (271 mg, 1.48 × $10^{-3}$ mol) in 10 mL of THF was added dropwise *n*-BuLi in hexanes (0.64 mL, 2.3 M, 1.47 × $10^{-3}$ mol) at 25 °C over 5 min. The resulting lithium amide solution was stirred for 10 min, and then $Cp_2Zr(CH_2CH_2CMe_3)(Cl)$ (482 mg, 1.41 × $10^{-3}$ mol, 0.95 equiv) was added. After 12 h at 25 °C the volatile materials were removed under reduced pressure, the remaining yellow solid was extracted with 20 mL of ether, and the solution was filtered to remove LiCl. The filtrate was collected, the volume was reduced to 5 mL under vacuum, and the solution was cooled to −30 °C. Over several days white crystals of **2e** grew and were isolated by filtration to yield 510 mg (1.04 × $10^{-3}$ mol, 74%). IR (Nujol): 3332 (w), 1491 (s), 1359 (s), 1310, 1264, 1235, 1170, 1082, 1057, 1026, 1017, 10023, 796 (s), 766, 737, 722, 699, 676, 622, 612 cm$^{-1}$. Anal. Calcd for $C_{29}H_{35}NZr$: C, 71.26; H, 7.22; N, 2.87. Found: C, 71.09; H, 7.26; N, 2.61.

**$Cp_2Zr(NH(4\text{-}CMe_3C_6H_4))_2$ (3a). From $Cp_2ZrCl_2$.** To 10 mL of THF containing 4-*tert*-butylaniline (426 mg, 2.85 × $10^{-3}$ mol) was added 1.24 mL of 2.3 M *n*-BuLi in hexanes (2.85 × $10^{-3}$ mol) via syringe at 25 °C. The solution was stirred for 5 min followed by addition of $Cp_2ZrCl_2$ (379 mg, 1.30 × $10^{-3}$ mol). The reaction mixture turned bright yellow upon addition of $Cp_2ZrCl_2$ and was stirred for 12 h. The solvent was then removed under reduced pressure and the remaining yellow powder extracted into 10 mL of toluene. The mixture was filtered and concentrated under vacuum to 3 mL. The solution was layered with 2 mL of hexanes and cooled to −30 °C. Yellow crystals which formed over several days were isolated by decanting the solvent away and washing the crystals with hexanes. This procedure yielded 557 mg (1.08 × $10^{-3}$ mol, 83%) of the bis(amide) **3a** which was judged pure by $^1$H NMR.

**From $Cp_2ZrMe_2$.** $Cp_2ZrMe_2$ (158 mg, 6.28 × $10^{-4}$ mol) and 4-*tert*-butylaniline (369 mg, 2.47 × $10^{-4}$ mol, 3.93 equiv) were dissolved in 7 mL of toluene and transferred to a glass bomb. The reaction vessel was degassed and heated to 105 °C for 72 h. The volatile materials were removed under reduced pressure, leaving a yellow solid which was dissolved in 2 mL of toluene, layered with 3 mL of hexanes, and cooled to −30 °C. Yellow crystals of **3a** were isolated by filtration to provide 271 mg (5.23 × $10^{-4}$ mol, 83%) of the bis(amide). IR ($C_6H_6$): 3353 (w), 2962, 1587, 1507, 1429, 1365, 1296, 1221, 1188, 1014, 908, 858, 831, 807, 732. MS (EI): *m/e* 518 ($M^+$), 134 (base). Anal. Calcd for $C_{26}H_{30}N_2Zr$: C, 69.58; H, 7.40; N, 5.41. Found: C, 69.21; H, 7.29; N, 5.22.

**$Cp_2Zr(NHCMe_3)_2$ (3b).** $Cp_2ZrMe_2$ (264 mg, 1.05 × $10^{-3}$ mol) was dissolved in 10 mL of toluene and transferred to a glass bomb. The solution was degassed and 0.80 mL of *tert*-butylamine (7.61 × $10^{-3}$ mol, 7.25 equiv) was added by vacuum transfer from a graduated bomb. The reaction vessel was heated at 150 °C for 4 days, after which the volatile materials were removed under reduced pressure to provide a light yellow solid. The solid was dissolved in 4 mL of hexanes and cooled to −30 °C. Light yellow crystals of the bis(amide) formed over several days and were recovered by filtration to provide 235 mg (6.43 × $10^{-4}$ mol, 61%) of **3b**. IR ($C_6H_6$): 3337 (w), 1679 (w), 1582 (w), 1354, 1209, 1200, 1019, 971, 810, 781, 770, 759 cm$^{-1}$. MS (EI): *m/e* 366 ($M^+$), 58 (base). Anal. Calcd for $C_{18}H_{30}N_2Zr$: C, 59.12; H, 8.27; N, 7.66. Found: C, 58.98; H, 8.14; N, 7.57.

**$Cp_2Zr(NH(2,6\text{-}Me_2C_6H_3))_2$ (3c). From $Cp_2ZrCl_2$.** 2,6-Dimethylaniline (2.96 g, 2.44 × $10^{-2}$ mol) was dissolved in 100 mL of THF. To this was added 9.8 mL of a 2.3 M (2.25 × $10^{-2}$ mol) solution of *n*-BuLi in hexanes at 25 °C. After the solution cooled, $Cp_2ZrCl_2$ (3.13 g, 1.07 × $10^{-2}$ mol) was added and the reaction mixture rapidly turned yellow. The solution was stirred for 3 h, and then the volatile materials were removed under reduced pressure. Then 80 mL of toluene was added, and the resulting slurry was stirred for 12 h. The slurry was filtered to remove the LiCl, the filtrate was collected, and the toluene was removed under reduced pressure. The remaining solid was washed with 3 × 20 mL of ether, leaving 3.53 g (7.64 × $10^{-3}$ mol, 71%) of yellow bis(amide) which was pure by $^1$H NMR.

**From $Cp_2ZrMe_2$.** A glass bomb was charged with $Cp_2ZrMe_2$ (163 mg, 6.48 × $10^{-4}$ mol), 2,6-dimethylaniline (320 mg, 2.64 × $10^{-4}$ mol, 4.08 equiv), and 10 mL of toluene. The bomb was degassed and heated for 48 h at 140 °C during which time the solution became yellow. The volatile materials were removed under reduced pressure, and the remaining solid was taken up in 3 mL of THF. The solution was layered with 2 mL of hexanes and cooled to −30 °C. Yellow crystals formed over several days and were collected by filtration to yield 252 mg (5.46 × $10^{-4}$ mol, 85% yield) of the bis(amide). IR ($C_6H_6$): 3345 (w), 1590, 1423, 1276, 1253, 1217, 1096, 910, 856, 811, 763, 741. MS (EI): *m/e* 462 ($M^+$), 121 (base). Anal. Calcd for $C_{30}H_{38}N_2Zr$: C, 67.63; H, 6.55; N, 6.07. Found: C, 67.54; H, 6.55; N, 6.01.

**$Cp_2Zr(NHSi(CMe_3)Me_2)_2$ (3d).** A glass bomb was charged with $Cp_2ZrMe_2$ (506.3 mg, 2.01 × $10^{-3}$ mol), $H_2NSi(CMe_3)Me_2$ (900 mg, 6.87 × $10^{-3}$ mol, 3.4 equiv), and 20 mL of benzene. The solution was degassed and heated at 140 °C for 3 days. The volatile materials were removed under reduced pressure, and the product was recrystallized from 8 mL of pentane layered with hexamethyldisiloxane at −30 °C to give clear needles of the bis(amide) **3d** which formed over several days and were recovered by decanting the solvent to yield 651.5 mg (1.36 × $10^{-3}$ mol, 68%). We were unable to detect an N–H stretching absorption for **3d**. IR (Nujol): 1465, 1458, 1453, 1377, 1250, 1064, 1016, 891, 853, 797 cm$^{-1}$. Anal. Calcd for $C_{22}H_{42}N_2Si_2Zr$: C, 54.82; H, 8.78; N, 5.81. Found: C, 54.86; H, 8.96; N, 5.73.

**$[Cp_2ZrN(4\text{-}CMe_3C_6H_4)]_2$ (4a).** A bomb was loaded with $Cp_2ZrMe_2$ (345 mg, 1.41 × $10^{-3}$ mol), 4-*tert*-butylaniline (2.11 mg, 1.41 × $10^{-3}$ mol), and 7 mL of toluene. The solution was degassed and heated to 105 °C for 48 h, during which time the solution became kelly-green. The reaction vessel was allowed to cool to room temperature over 1 day during which time large kelly-green hexagonal crystals formed and were isolated by decanting the solvent to furnish 363 mg (4.92 × $10^{-4}$ mol, 70%) of the imido dimer **4a**. When the reaction was run in a sealed NMR tube in $C_6D_6$ under identical conditions, methane (δ 0.15) was identified as a product of this reaction by $^1$H NMR spectrometry. Due to the insolubility of **4a** we were unable to recrystallize it and obtain a satisfactory elemental analysis.

**Cp$_2$Zr(NCMe$_3$)(THF) (5b).** In the drybox Cp$_2$Zr(NHCMe$_3$)(Me) was prepared using 218 mg ($8.02 \times 10^{-4}$ mol) of Cp$_2$Zr(Me)(Cl). The methyl amide **2b** was loaded into a bomb with 10 mL of THF, and the solution was degassed and heated for 3 days at 85 °C. The solvent was removed under reduced pressure to leave a yellow solid which was dissolved in 4 mL of toluene, and the resulting solution was layered with 3 mL of hexanes and cooled to −30 °C. Translucent yellow crystals formed over several days and were recovered by decanting the solvent to provide 208 mg ($5.70 \times 10^{-4}$ mol, 71%) of the monomeric imido complex **5b**. IR (C$_6$H$_6$): 2954, 2930, 2846, 2711, 2075, 1450, 1359, 1344, 1238 (s), 1205, 1125, 1105, 918, 874, 773, 515 cm$^{-1}$. Anal. Calcd for C$_{18}$H$_{27}$NOZr: C, 59.29; H, 7.46; N, 3.84. Found: C, 59.50; H, 7.45; N, 3.81.

**Cp$_2$Zr(N(2,6-Me$_2$C$_6$H$_3$)(THF) (5c).** A bomb was charged with Cp$_2$Zr(NH(2,6-Me$_2$-C$_6$H$_3$))(CH$_2$CH$_2$CMe$_3$) (560 mg, $1.32 \times 10^{-3}$ mol) in 10 mL of THF. The solution was degassed and heated for 10 days at 85 °C, and the volatile materials were removed to yield an orange solid. This residue was extracted into 6 mL of toluene, and the resulting mixture was cooled to −30 °C. Orange needles of Cp$_2$Zr(N(2,6-Me$_2$C$_6$H$_3$))(THF) formed over several days and were recovered by filtration and washed with 3 mL of cold hexanes to provide 374 mg ($9.04 \times 10^{-4}$ mol, 69%) of the imido complex **5c**. IR (C$_6$H$_6$): 2979, 2957, 2949, 2933, 2901, 2361, 2339, 1684, 1653, 1585, 1577, 1546, 1457 (s), 1436, 1406, 1367, 1314, 1094, 1019, 913, 869, 784 (s), 774, 554, 504, 492, 483, 472, 467, 406 (s) cm$^{-1}$. Anal. Calcd for C$_{22}$H$_{27}$NOZr: C, 64.03; H, 6.59; N, 3.39. Found: C, 63.64; H, 6.65; N, 3.34.

**Cp$_2$Zr(NSi(CMe$_3$)Me$_2$)(THF) (5d).** A glass bomb was charged with Cp$_2$Zr(NHSi(CMe$_3$)Me$_2$)(CH$_2$CH$_2$CMe$_3$) (51.9 mg, $1.18 \times 10^{-4}$ mol) and 6 mL of THF. The bomb was degassed and heated for 32 h at 85 °C, after which the solution was clear brown. The volatile materials were removed under reduced pressure, leaving a brown oil which was dissolved in 3 mL of toluene, and the resulting solution layered with 2 mL of pentane and cooled to −30 °C. Under these conditions large clear crystals formed over several days and were isolated by decanting the solvent and washing the crystals with 2 mL of cold pentane to provide 36.3 mg ($8.59 \times 10^{-5}$ mol, 72%) of **5d**. IR (Nujol): 1455 (s), 1378, 1354, 1264, 1231, 1069, 1037, 1017, 1007, 894, 867, 821, 783, 742, 707, 658, 514 cm$^{-1}$. Anal. Calcd for C$_{20}$H$_{33}$NOSiZr: C, 56.82; H, 7.87; N, 3.31. Found: C, 56.93; H, 7.93; N, 3.46.

**Cp$_2$Zr(NCMe$_3$)(OPPh$_3$) (6b).** To a stirred solution of Cp$_2$Zr(NCMe$_3$)(THF) (109 mg, $3.00 \times 10^{-4}$ mol) in 20 mL of toluene was added triphenylphosphine oxide (83.5 mg, $3.00 \times 10^{-4}$ mol) at 25 °C. The color of the solution turned a brighter shade of yellow upon addition of the phosphine oxide. After 30 min the volume of solvent was reduced to 4 mL by evaporation under vacuum. The solution was layered with 3 mL of hexanes and cooled to −30 °C. Large bright yellow crystals of **6b** formed over several days and were isolated by decanting the solvent to yield 158 mg ($2.76 \times 10^{-4}$ mol, 92%). $^{31}$P{$^1$H} NMR: $\delta$ 41.78. IR (C$_6$H$_6$): 2952, 2928, 1439, 1343, 1239, 1202, 1175, 1123, 1097, 770, 727 cm$^{-1}$. MS (EI): *m/e* 569 (m$^+$), 58 (base). Anal. Calcd for C$_{32}$H$_{34}$NOPZr: C, 67.33; H, 6.00; N, 2.45. Found: C, 67.29; H, 6.01; N, 2.41.

**Cp$_2$Zr(NHCMe$_3$)(Ph) (7b).** A glass bomb was charged with Cp$_2$Zr(NHCMe$_3$)(Me) (700 mg, $2.27 \times 10^{-3}$ mol) and 15 mL of C$_6$H$_6$. The solution was degassed and heated at 85 °C for 42 h, after which the volatile materials were removed under vacuum. The remaining yellow solid was dissolved in 3 mL of toluene, and the solution was layered with 2 mL of hexanes and cooled to −30 °C. Under these conditions clear crystals of **7b** formed over several days and were isolated by filtration to provide 514 mg ($1.39 \times 10^{-3}$ mol, 61%). IR (C$_6$H$_6$): 3299 (w), 2960, 2729, 1445, 1414, 1374, 1358, 1203, 980, 914, 800, 723 cm$^{-1}$. Anal. Calcd for C$_{20}$H$_{25}$NZr: C, 64.81; H, 6.80; N, 3.78. Found: C, 64.62; H, 6.82; N, 3.66.

**Cp$_2$Zr(NH(2,6-Me$_2$C$_6$H$_3$))(Ph) (7c).** A bomb was loaded with Cp$_2$ZrPh$_2$ (125 mg, $3.34 \times 10^{-4}$ mol), 2,6-dimethylaniline (80.8 mg, $6.67 \times 10^{-4}$ mol, 2.0 equiv), and 10 mL of C$_6$H$_6$. The solution was degassed and heated with stirring at 85 °C for 3 h, and then the solvent was removed under reduced pressure. The remaining yellow solid was dissolved in 1 mL of toluene, and hexanes were vapor diffused in at −30 °C. Fluffy yellow crystals formed over several days and were recovered by filtration to provide 88.1 mg ($2.10 \times 10^{-4}$ mol, 63% yield) of **7c**. IR (C$_6$H$_6$): 3295 (w), 1214, 1018, 806, 766, 723, 703, 464, 452 cm$^{-1}$. Anal. Calcd for C$_{24}$H$_{25}$NZr: C, 68.85; H, 6.02; N, 3.35. Found: C, 68.54; H, 5.89; N, 3.21.

**Cp$_2$Zr(NHSi(CMe$_3$)Me$_2$)(Ph) (7d).** A bomb was loaded with Cp$_2$Zr(NHSi(CMe$_3$)Me$_2$)(CH$_2$CH$_2$CMe$_3$) (321 mg, $7.49 \times 10^{-4}$ mol) and 10 mL of C$_6$H$_6$. The solution was degassed and heated to 95 °C for 28 h, after which the volatile materials were removed under reduced pressure. The remaining brown solid was dissolved in 7 mL of a 2:5 mixture of toluene/hexamethyldisiloxane, and the solution was cooled to −30 °C. White crystals formed over several days and were isolated by decanting the solvent to yield 181 mg of **7d** ($4.40 \times 10^{-4}$ mol, 59%). IR (Nujol): 3325 (w), 3046, 2895 (s), 2881 (s), 1468, 1443, 1386, 1361, 1253, 1247, 1088, 1056, 1016, 868, 826, 799, 737, 722, 702, 665 cm$^{-1}$. Anal. Calcd for C$_{22}$H$_{31}$NSiZr: C, 61.62; H, 7.29; N, 3.27. Found: C, 61.87; H, 7.31; N, 3.16.

**Cp$_2$Zr(N(CMe$_3$)CHCPh) (10b).** The imido complex Cp$_2$Zr(NCMe$_3$)(THF) (106 mg, $2.91 \times 10^{-4}$ mol) was dissolved in 5 mL of toluene, and phenylacetylene (37.1 mg, $3.63 \times 10^{-4}$ mol, 1.25 equiv) was added at 25 °C. Upon addition of the phenylacetylene the solution turned purple within seconds. After 10 min the volatile components were removed under reduced pressure and an NMR sample was prepared. The $^1$H NMR spectrum of the crude reaction mixture exhibited resonances for only one oganometallic product, the metallacycle **10b**. The NMR sample was added to the remaining solid, and the solvent was removed under vacuum. The combined solids were dissolved in a mixture of toluene (0.5 mL) and pentane (2 mL) and cooled to −30 °C. Purple wedge-shaped crystals of **10b** formed over 1 day and were isolated by decanting off the solvent to yield 73 mg ($1.85 \times 10^{-4}$ mol, 51%). IR (Nujol): 1498, 1484, 1358, 1291, 1213 (s), 1135, 1014, 791 (s), 749, 692, 629 cm$^{-1}$. Anal. Calcd for C$_{22}$H$_{25}$NZr: C, 66.95; H, 6.38; N, 3.55. Found: C, 67.24; H, 6 69; N, 3.70.

**Determination of the Regiochemistry of 10b.** In the drybox crystals of the metallacycle **10b** (9.2 mg, $2.33 \times 10^{-5}$ mol) were dissolved in 1.0 mL of C$_6$H$_6$, and in air 1 mL of 5% HCl was immediately added to the solution of the metallacycle. Upon addition of the HCl the color of the solution changed from purple to yellow and finally to clear within 1 min. A sample of the organic layer was analyzed by GCMS. A single peak detected by GC was determined by mass spectrometry to have parent (120 amu) fragmentation pattern and retention identical to those of commercially available phenylacetaldehyde (base 65). Analysis of a sample of acetophenone by GCMS exhibited a different retention time and mass spectral fragmentation pattern (parent 120, base 105).

**C$_{21}$H$_{29}$NZr (12b).** A flask was loaded with the imido complex **5b** (63.3 mg, $1.74 \times 10^{-4}$ mol), norbornene (503 mg, $5.34 \times 10^{-3}$ mol, 31 equiv) and 4 mL of hexanes. The resulting solution was stirred at 25 °C until all of the imido complex had dissolved (1 h), leaving an orange solution of the metallacycle **12b**. The volatile materials were then removed, and a portion of the reaction mixture was dissolved in C$_6$D$_6$. The $^1$H NMR spectrum indicated clean conversion to the metallacycle **12b**. Attempts to crystallize this material led to low yields due to its high solubility. However, eventually three crystals were grown from hexamethyldisiloxane after 6 months at −30 °C and were used for the structure determination. The product was typically obtained as an orange powder from 2 mL of hexamethyldisiloxane to provide 31 mg ($8.00 \times 10^{-4}$ mol, 46%) of **12b**. This material was not of suitable purity for elemental analysis. IR (neat film): 2958, 2869, 1445, 1353, 1207, 1014 (s) cm$^{-1}$.

**Reaction of Ethylene with Cp$_2$Zr(NCMe$_3$)(THF): Formation of 13b.** A 22-cm Wilmad PS 505 NMR tube was charged with Cp$_2$Zr(NCMe$_3$)(THF) (28 mg, $7.68 \times 10^{-5}$ mol) and 0.6 mL of toluene-$d_8$. The NMR tube was fitted with a vacuum adapter and the solution was degassed on a vacuum line. Ethylene (238 Torr) was transferred from a 29-mL volumetric bulb ($3.71 \times 10^{-4}$ mol, 4.8 equiv) into the NMR tube by cooling the tube to −196 °C. The tube was then flame sealed. As it thawed, the solution turned a slightly brighter shade of yellow. Integration of the $^1H$ NMR spectrum showed that 38% of the imido complex had been converted to **13b** under these conditions and that 3.7 equiv of ethylene remained in solution. Using these data the equilibrium constant was determined to be 0.07 ± 0.008 at 25 °C.

**$Cp_2Zr(N(CMe_3)C{=}NCMe_3)(CNCMe_3)$ (16).** A bomb was charged with the monomeric imido complex $Cp_2Zr(NCMe_3)(THF)$ (144 mg, $3.95 \times 10^{-4}$ mol) and 5 mL of toluene. The solution was degassed and frozen, and then *tert*-butyl isocyanide ($1.18 \times 10^{-3}$ mol, 3 equiv) was added by vacuum transfer from a known volume bulb. As the solution was thawed, the color changed from faint to bright yellow and a precipitate formed. After 20 min at room temperate the volatile materials were removed under vacuum, leaving a yellow solid. This was dissolved in 3 mL of THF, and ether was vapor diffused into the solution at −30 °C. Yellow needles of **16** formed after several days and were isolated from the solution by decanting to yield 147 mg of **16** ($3.20 \times 10^{-4}$ mol, 81%). IR (THF): 2186 (s), 1570 (s), 794 $cm^{-1}$. MS (FAB, sulfolane): 458 ($MH^+$). Anal. Calcd for $C_{24}H_{37}N_3Zr$: C 62.83; H, 8.13; N, 9.16. Found: C, 62.49; H, 7.95; N, 9.15.

**$Cp_2Zr(NHCMe_3)(OCH_2C({=}CH_2)CH_3)$ (17).** A bomb was charged with the imido complex **5b** (125 mg, $3.43 \times 10^{-4}$ mol) and 10 mL of toluene. The solution was degassed and frozen by cooling to −196 °C and isobutylene oxide ($5.15 \times 10^{-4}$ mol, 1.5 equiv) transferred into the bomb by vacuum transfer from a known volume bulb. The reaction mixture was thawed and allowed to stand for 20 min, and the volatile materials were removed under vacuum. The $^1H$ NMR spectrum of the remaining solid indicated that the product was >95% pure; however, attempts to crystallize this material led to intractable products. IR ($C_6H_6$): 3338 (w), 2953, 2906, 2888, 1654 (w), 1365, 1206, 1135, 1120, 793 $cm^{-1}$.

**$Cp_2Zr(N(CHPh_2)CPhCPh)$ (19e).** $Cp_2Zr(NHCHPh_2)(CH_2CH_2CMe_3)$ (197 mg, $4.03 \times 10^{-4}$ mol), diphenylacetylene (287 mg, $1.61 \times 10^{-3}$ mol, 4.0 equiv), and 10 mL of $C_6H_6$ were loaded into a glass bomb. The solution was degassed and heated to 115 °C for 24 h, during which time the solution turned green-brown. After removal of the volatile materials under reduced pressure the remaining solid was washed with hexanes (3 × 10 mL) until the hexanes remained clear, leaving a bright green solid. The solid was dissolved in 5 mL of toluene, and the solution was layered with 3 mL of hexanes and cooled to −30 °C. Under these conditions green crystals of the metallacycle **19e** formed over several days and were isolated by filtration to provide 150 mg ($2.58 \times 10^{-4}$ mol, 64%). IR (Nujol): 2726, 2671, 1585, 1502, 1455 (s), 1451 (s), 1341, 1300, 1284, 1263, 1221, 1176, 1120, 1072, 1016, 794, 781, 766, 722, 701 $cm^{-1}$. We were unable to get satisfactory elemental analysis on this compound despite repeated attempts. The recrystallized compound was determined to be >98% pure by $^1H$ NMR spectrometry.

**Reaction of $Cp_2Zr(NCMe_3)(THF)$ with Benzophenone.** Two solutions were prepared. The first contained benzophenone (6.1 mg, $3.35 \times 10^{-5}$ mol) and ferrocene (5.8 mg, $3.12 \times 10^{-5}$ mol) as internal standard dissolved in 0.5 mL of $C_6D_6$, and the other contained $Cp_2Zr(NCMe_3)(THF)$ (11.2 mg, $3.07 \times 10^{-5}$ mol) also in 0.5 mL of $C_6D_6$. The solutions were combined at room temperature, and upon mixing, a white precipitate (presumably oligiomeric zirconocene oxide) formed. Analysis by $^1H$ NMR spectrometry showed that the *tert*-butylimine of benzophenone[51] (**14**) was formed in 89% yield, as determined by integration against the ferrocene internal standard. The reaction mixture was run through a pipet of silica and injected into a GCMS. The imine **14** was also identified by GCMS: MS (EI) $M^+$, 236 (base, 222).

**Reaction of $Cp_2Zr(NCMe_3)(THF)$ with *tert*-Butyl Isocyanate.** An NMR tube was loaded with $Cp_2Zr(NCMe_3)(THF)$ (16.5 mg, $4.53 \times 10^{-5}$ mol), *p*-dimethoxybenzene (as an NMR internal standard) and $C_6D_6$. The NMR tube was fitted with a vacuum adapter, and the solution was degassed and cooled to −196 °C. The *tert*-butyl isocyanate ($6.34 \times 10^{-5}$ mol, 1.4 equiv) was added to the frozen solution by vacuum transfer from a known volume bulb and the NMR tube was then flame sealed. Upon thawing, a white precipitate formed (presumably oligomeric zirconocene oxides). $^1H$ NMR spectrometry indicated that 1,3-di-*tert*-butylcarbodiimide (**15**) (s, 1.16 ppm in $C_6D_6$) was formed in 65% yield by integration against the internal standard. The $^1H$ NMR and GCMS data for the 1,3-di-*tert*-butylcarbodiimide were identical to those of an authentic sample purchased from Aldrich.

**Thermolysis of $Cp_2Zr(NCMe_3)(THF)$ in $C_6D_6$.** An NMR tube was charged with the monomeric imido complex **5b** (9.9 mg, $2.71 \times 10^{-5}$ mol), cyclohexane (as the NMR internal standard), and 0.6 mL of $C_6D_6$. The solution was degassed, the NMR tube was flame sealed, and two initial one-pulse $^1H$ NMR spectra were acquired in which the resonances of **5b** were integrated against the cyclohexane. The solution was heated to 85 °C and the reaction monitored by $^1H$ NMR spectrometry. The half-life was determined to be ~45 min under these conditions. After 5 h another $^1H$ NMR spectrum was taken as described above. In this manner the reaction was determined to provide a 94% yield of **7b** which was identified by the chemical shifts of the *tert*-butyl and cyclopentadienyl groups and their relative integrations (9H to 10H).

**Reaction of $Cp_2Zr(C_6H_4)(PMe_2Ph)$ with $H_2NSi(CMe_3)Me_2$: Independent Synthesis of 7d.** An NMR tube was charged with the benzyne complex[17] $Cp_2Zr(C_6H_4)(PMe_2Ph)$ (8.7 mg, $2.00 \times 10^{-5}$ mol), *p*-dimethoxybenzene (2.8 mg, $2.03 \times 10^{-5}$ mol) as the NMR internal standard, and 0.6 mL of $C_6D_6$. Two single-pulse $^1H$ NMR spectra were acquired in which the resonance of the cyclopentadienyl ligands was integrated against the methyl resonance of the *p*-dimethoxybenzene. The amine $H_2NSi(CMe_3)Me_2$ (5.8 mg, $4.42 \times 10^{-5}$ mol, 2.2 equiv) was added to the NMR tube at 25 °C, and after 10 min two $^1H$ NMR spectra were obtained as described above. Using this technique it was determined that the phenyl amide $Cp_2Zr(NHSi(CMe_3)Me_2)(Ph)$ was formed in 89% yield.

**Reaction of 2,6-Dimethylaniline with $Cp_2Zr(N(2,6\text{-}Me_2C_6H_3))(THF)$.** An NMR tube was charged with $Cp_2Zr(N(2,6\text{-}Me_2C_6H_3))(THF)$ (6.5 mg, $1.57 \times 10^{-5}$ mol), *p*-dimethoxybenzene (1.5 mg, $1.08 \times 10^{-5}$ mol), and 0.6 mL of $C_6D_6$. Two single-pulse $^1H$ NMR spectra were acquired in which the resonance of the cyclopentadienyl ligands was integrated against the methyl resonance of the *p*-dimethoxybenzene. 2,6-Dimethylaniline (5.8 mg, $4.78 \times 10^{-5}$ mol, 3.0 equiv) was added to the NMR tube at 25 °C, and the color of the solution changed from orange to yellow in less than 2 min. After 20 min another set of $^1H$ NMR spectra were obtained as described above. When the integrated areas were averaged, it was determined that **3a** was formed in >98% yield.

**X-ray Diffraction Study of $[Cp_2Zr(N(4\text{-}CMe_3\text{-}C_6H_4))]_2$ (4a).** Large clear green crystals of compound **4a** were obtained by slow cooling of the toluene reaction solution after thermolysis of $Cp_2ZrMe_2$. Fragments cleaved from some of these crystals were mounted on glass fibers using polycyanoacrylate cement and then coated with epoxy to protect them from the atmosphere. Preliminary precession photographs indicated monoclinic Laue symmetry and yielded approximate cell dimensions.

The crystal used for data collection was then transferred to an Enraf-Nonius CAD-4 diffractometer and centered in the beam.[52] Automatic peak search and indexing procedures yielded a triclinic reduced primitive cell. Inspection of the Niggli values revealed no conventional cell of higher symmetry. The final cell parameters and specific data collection parameters for this data set are given in Table I.

The 2868 raw intensity data were converted to structure factor amplitudes and their esd's by correction for scan speed, background, and Lorentz and polarization effects. Inspection of the intensity standards revealed a reduction of 6% of the original intensity. The data were corrected for this decay. Inspection of

---

[51] Moretti, I.; Torre, G. *Synthesis* **1970**, 141.

[52] For a description of the X-ray diffraction and analysis protocols used, see: (a) Hersh, W. H.; Hollander, F. J.; Bergman, R. G. *J. Am. Chem. Soc.* **1983**, *105*, 5834. (b) Roof, R. B., Jr. A Theoretical Extension of Reduced-Cell Concepts in Crystallography. Publication LA-4038; Los Alamos Scientific Laboratory: Los Alamos, NM, 1969. (c) Cromer, D. T.; Waber, J. T. *International Tables for X-ray Crystallography*; Kynoch Press: Birmingham, England, 1974; Vol. IV, Table 2.2B.

the azimuthal scan data showed a variation $I_{min}/I_{max} = \pm 2\%$ for the average curve. No correction for absorption was applied. Inspection of the systematic absences indicate uniquely space group $P2_1/n$. Removal of systematically absent and redundant data left 2664 unique data in the final data set.

The structure was solved by Patterson methods and refined via standard least-squares and Fourier techniques. The disorder in the cyclopentadienyl rings, *tert*-butyl groups, and the toluene of solvation was resolved by inspection of Fourier and difference Fourier contour maps and by repeated tests of different models. Specific tests included refinement of the anisotropic thermal parameters for C9 and C9′ (found to be reasonable), comparison of a multiatom versus a six-atom disorder for Cp2 (the six atom model was much better), and comparison of large thermal motion versus partial occupancy for the toluene (the toluene seems to be full occupancy, but with substantial thermal motion).

The final residuals for 233 variables refined against the 2375 data for which $F^2 > 3\sigma(F^2)$ were $R = 4.28\%$, $R_w = 6.89\%$, and GOF = 3.74. The $R$ value for all 2664 data was 5.3%.

The quantity minimized by the least-squares program was $\sum w(|F_o| - |F_c|)^2$, where $w$ is the weight of a given observation. The $p$-factor, used to reduce the weight of intense reflections, was set to 0.03 throughout the refinement. The analytical forms of the scattering factor tables for the neutral atoms were used, and all scattering factors were corrected for both the real and imaginary components of anomalous dispersion.

Inspection of the residuals ordered in ranges of $(\sin\theta)/\lambda$, $|F_o|$, and parity and value of the individual indexes showed no unusual features or trends. The largest peak in the final difference Fourier map had an electron density of 0.85 e/Å$^3$, and the lowest excursion was −0.40/Å$^3$. There was some indication of the four hydrogens on the phenyl ring of the imido ligand, but it was felt that they were not worth including given the nature of the rest of the model. There was no indication of secondary extinction in the high-intensity low-angle data. The positional parameters of the non-hydrogen atoms are given in the supplementary material.

**X-ray Diffraction Study of $Cp_2Zr(NCMe_3)(THF)$ (5b).** Clear columnar crystals of compound **5b** were obtained by slow crystallization from diffusion of hexanes into toluene at −30 °C. Fragments cleaved from some of these crystals were mounted in thin-wall glass capillaries in a nitrogen atmosphere glovebox and then flame sealed. Preliminary precession photographs indicated orthorhombic Laue symmetry and yielded approximate cell dimensions. Automatic peak search and indexing procedures yielded the orthorhombic reduced primitive cell. The final cell parameters and specific data collection parameters for this data set are given in Table I.

Inspection of the systematic absences indicated possible space groups $Pna2_1$ or $Pnma$. These differ not only in the presence or absence of an inversion center but also in the interchange of the $b$ and $c$ axes. Since the cell volume was consistent with $Z = 4$, and we hoped for an ordered structure, the data collection proceeded for the setting $Pna2_1$. Successful solution and refinement of the structure, however, clearly indicate the correctness of the centric space group. Data were transformed to the setting for $Pnma$ and are reported as if collected in that setting.

The 2717 unique raw intensity data were converted to structure factor amplitudes and their esd's by correction for scan speed, background, and Lorentz and polarization effects. Inspection of the intensity standards revealed a nonlinear reduction of the standards to 86.3% of the original intensity. The data were corrected for this decay. Inspection of the azimuthal scan data showed a variation $I_{min}/I_{max} = 0.92$ for the average curve. An absorption correction based on the measured shape and size of the crystal and an 8 × 8 × 28 Gaussian grid of internal points was applied to the data ($T_{max} = 0.93$, $T_{min} = 0.91$) following a solution and partial refinement of the structure. Removal of systematically absent and averaging of redundant data ($R_{av}(I) = 2.4\%$) left 1290 unique data in the final data set.

The structure was solved by Patterson methods (in space group $Pna2_1$) and refined via standard least-squares and Fourier techniques in space group $Pnma$ following the discovery of the effective mirror plane. Just before the final cycles of refinement 10 reflections with anomalously large weighted residuals were removed from the data set. There was no evidence for reliable hydrogen atom positions in the final difference Fourier map, so hydrogens were not included in the structure factor calculations.

The final residuals for 109 variables refined against the 997 data for which $F^2 > 3\sigma(F^2)$ were $R = 1.63\%$, $R_w = 5.87\%$, and GOF = 1.925. The $R$ value for all 1290 data was 6.86%.

The largest peak in the final difference Fourier map had an electron density of 0.43 e/Å$^3$, and the lowest excursion was −0.26 e/Å$^3$. There was no indication of secondary extinction in the high-intensity low-angle data. The positional parameters of the non-hydrogen atoms are given in the supplementary material.

**X-ray Diffraction Study of 12b.** Pale orange crystals of compound **12b** were obtained by slow crystallization from hexamethyldisiloxane at −30 °C. Some of these crystals were mounted in thin-wall glass capillaries in a nitrogen atmosphere glovebox and then flame sealed.

Automatic peak search and indexing procedures yielded the triclinic reduced primitive cell. The final cell parameters and specific data collection parameters for this data set are given in Table I. The 2367 unique raw intensity data were converted to structure factor amplitudes and their esd's by correction for scan speed, background, and Lorentz and polarization effects. No correction for crystal decomposition was necessary. Inspection of the azimuthal scan data showed no empirical correction based on the observed variation was necessary. The structure was solved by Patterson methods and refined via standard least-squares and Fourier techniques. All atoms were refined with isotropic thermal parameters. The final residuals for 98 variables refined against the 2130 data for which $F^2 > 3\sigma(F^2)$ were $R = 6.1\%$, $R_w = 9.5\%$, and GOF = 4.83. The $R$ value for all 2367 data was 6.6%. The positional parameters of the non-hydrogen atoms are given in the supplementary material.

**Acknowledgment.** We are grateful for financial support of this work from the National Institutes of Health (Grant no. GM25459) and helpful discussions with Anne M. Baranger and Prof. Richard A. Andersen.

**Supplementary Material Available:** Tables of temperature factor expressions ($B$'s) and positional parameters with their estimated standard deviations (3 pages). Ordering information is given on any current masthead page.

OM9301344